

Physical processes and pattern formation in cloudy boundary layers

Christopher S. Bretherton

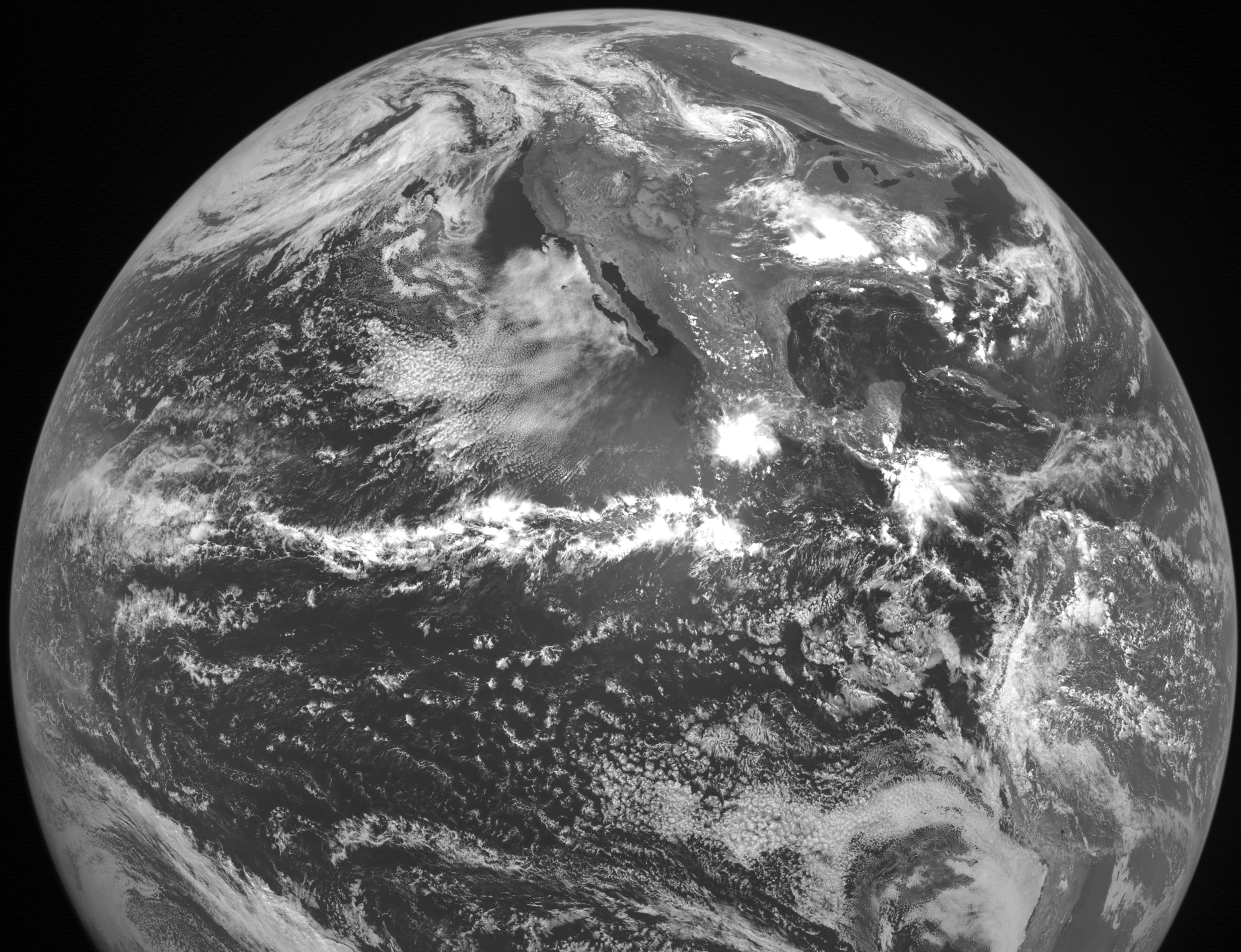
Peter Blossey and Xiaoli Zhou

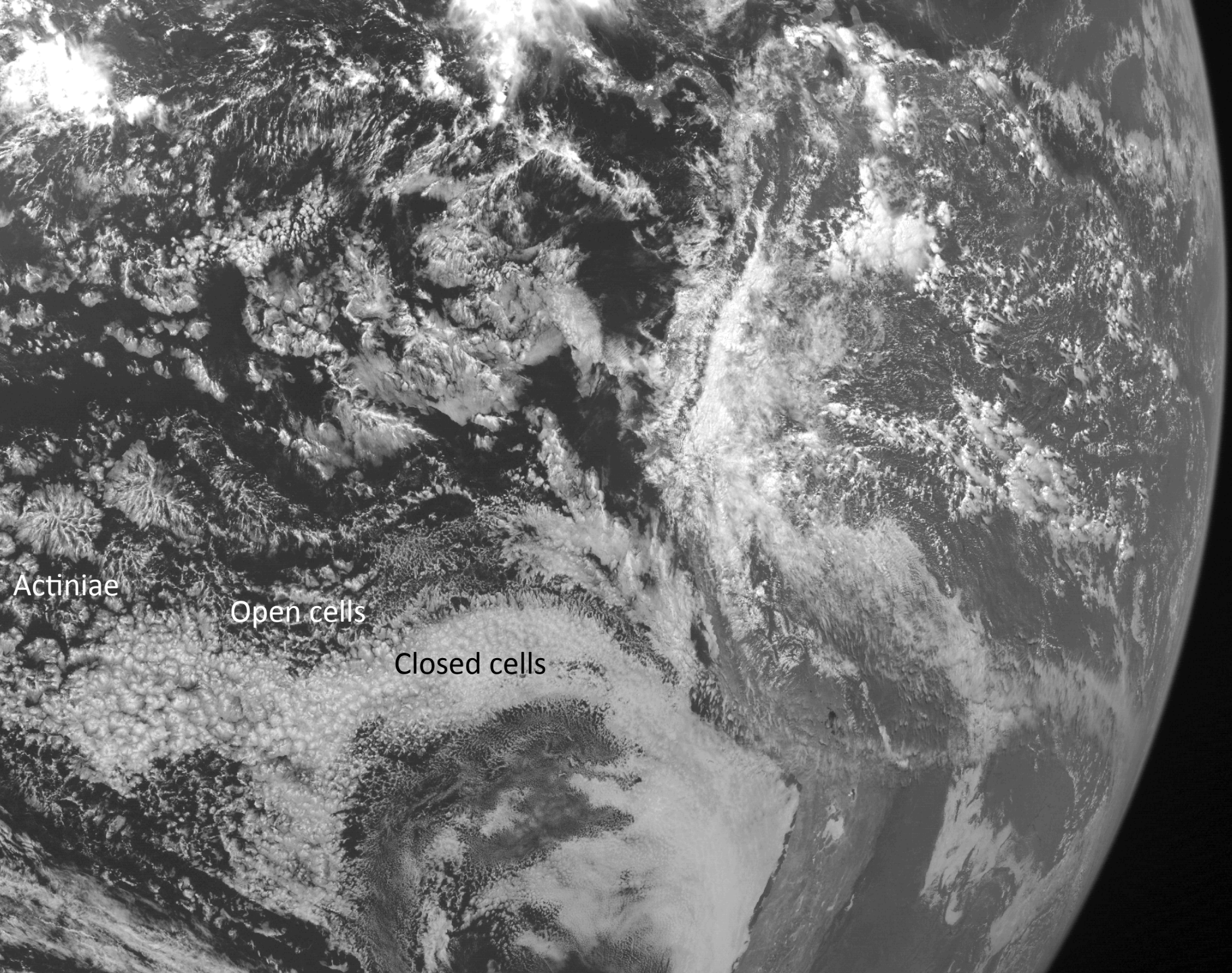
University of Washington Department of Atmospheric Sciences

*Bretherton and Blossey 2017 JAMES
Zhou and Bretherton 2018 JAS in prep*



Imagery





Actiniae

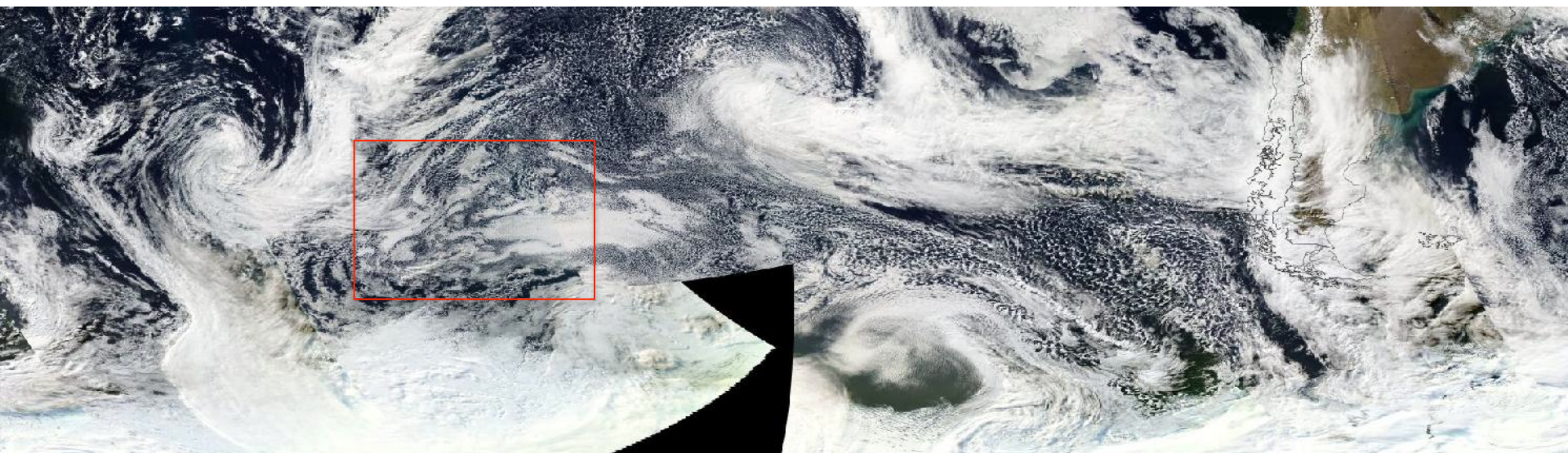
Open cells

Closed cells

Typical cloud patterns in the Southern Ocean

33S

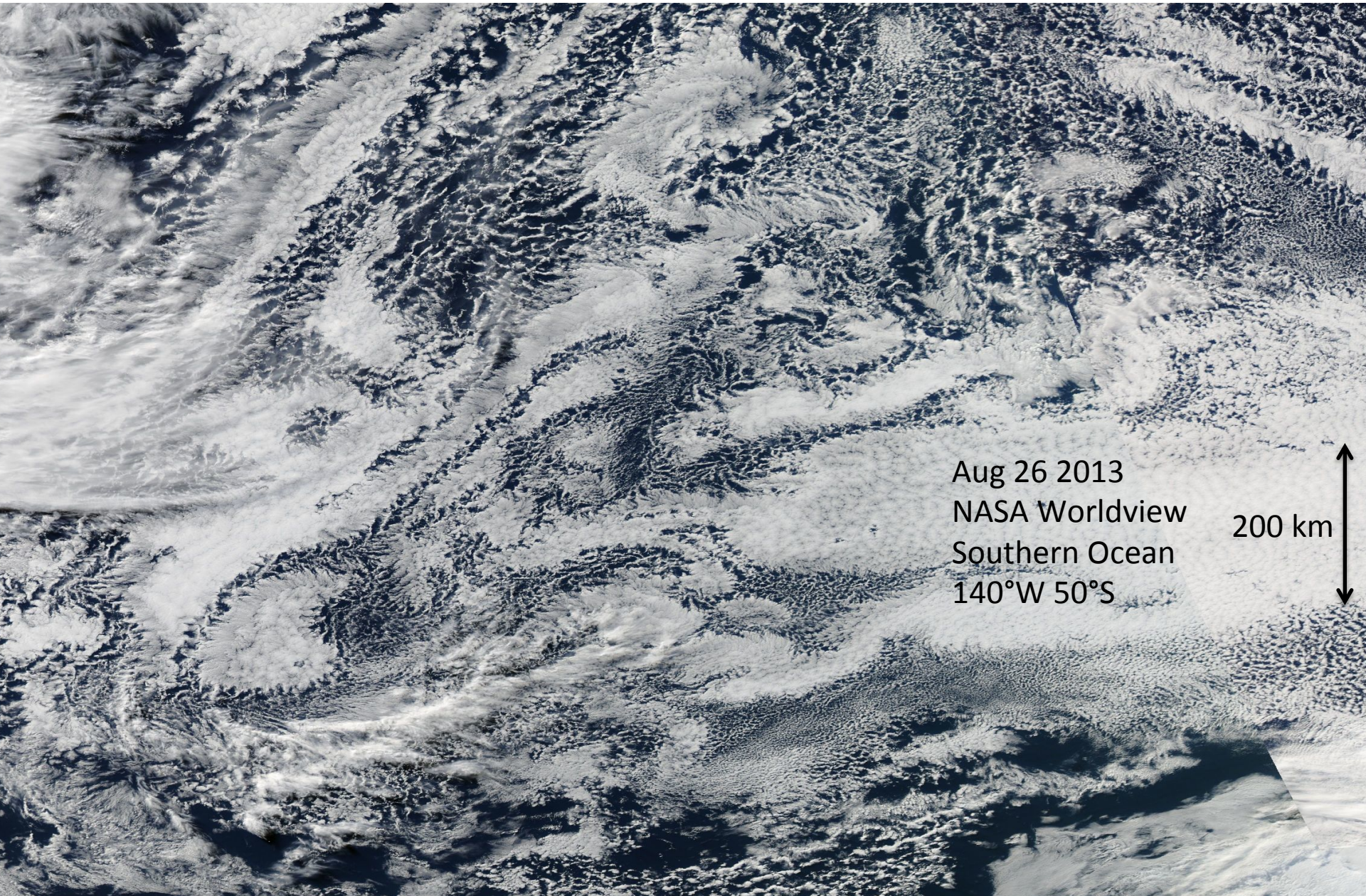
26 Aug 2013 Aqua composite ([NASA Worldview](#))



73S 180W

50 W

Open and closed cell mesoscale cellular convection (MCC)



Aug 26 2013
NASA Worldview
Southern Ocean
140°W 50°S

200 km

Non-polygonal cumulus clustering is also common

CSET RF04
12 July 2015

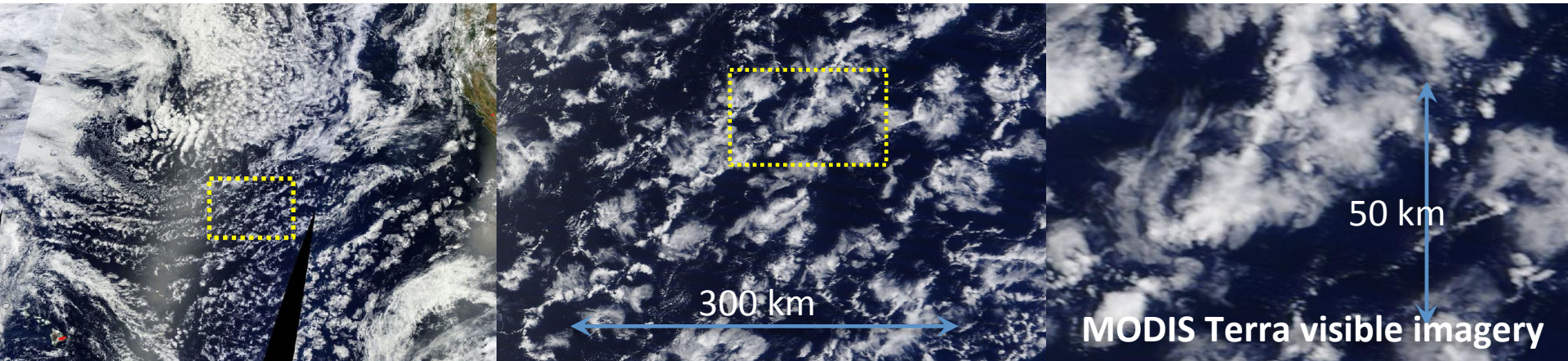
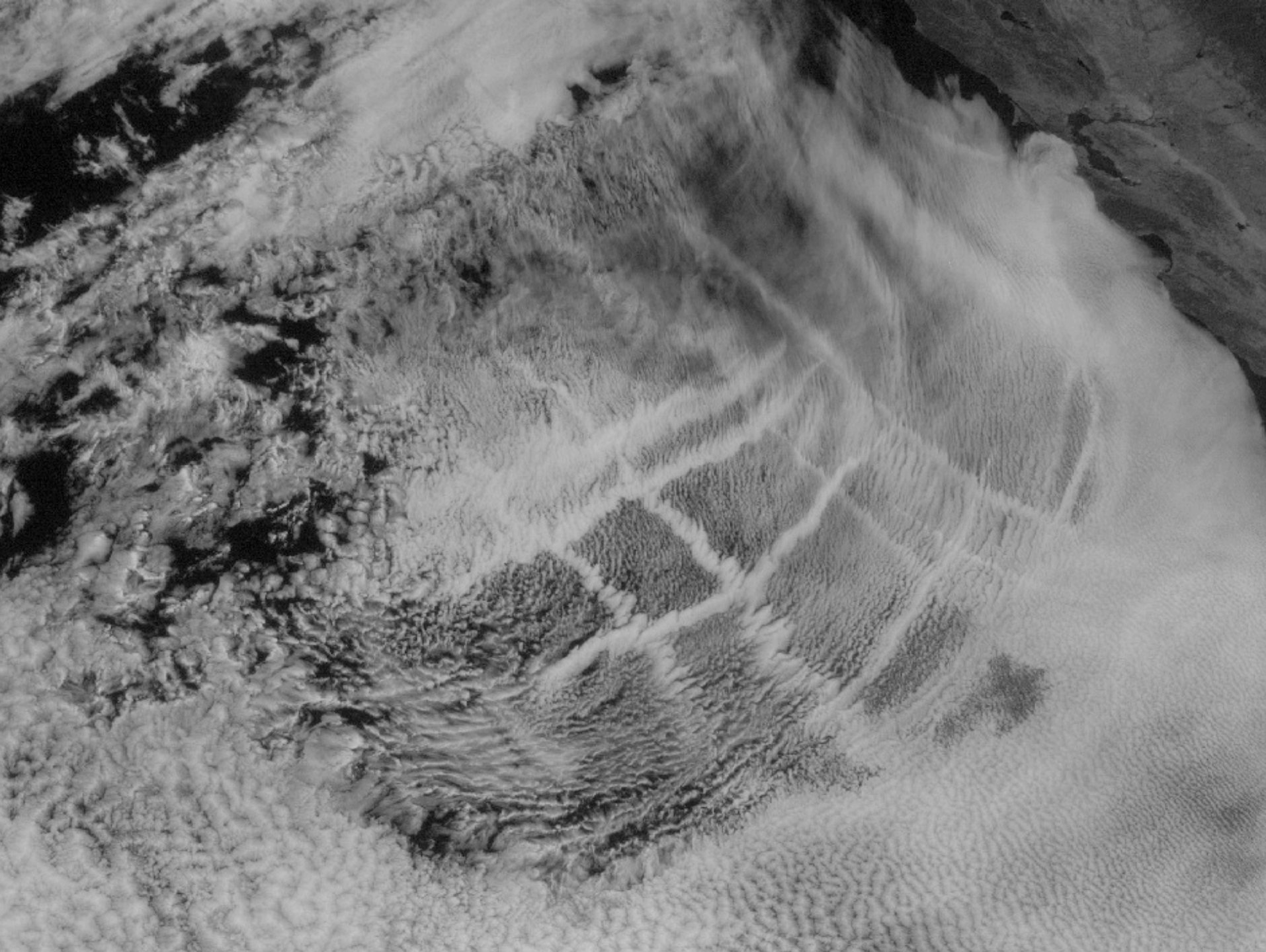
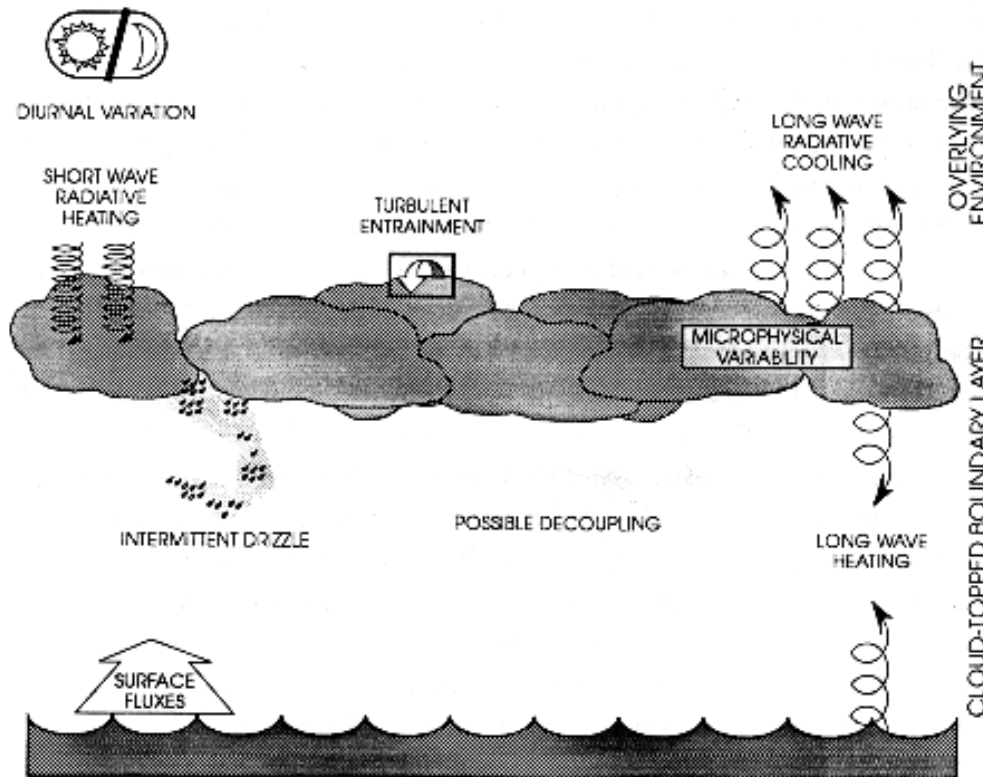


Photo: Bruce Albrecht

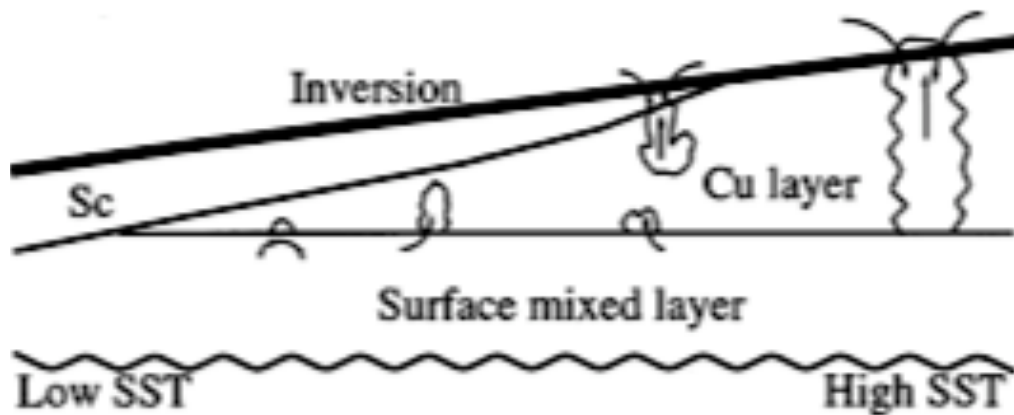


Observational analysis

Preamble: Physical processes affecting cloudy boundary layers



Siems et al. 1993



Wyant et al. 1997

Observations of mesoscale cellular convection

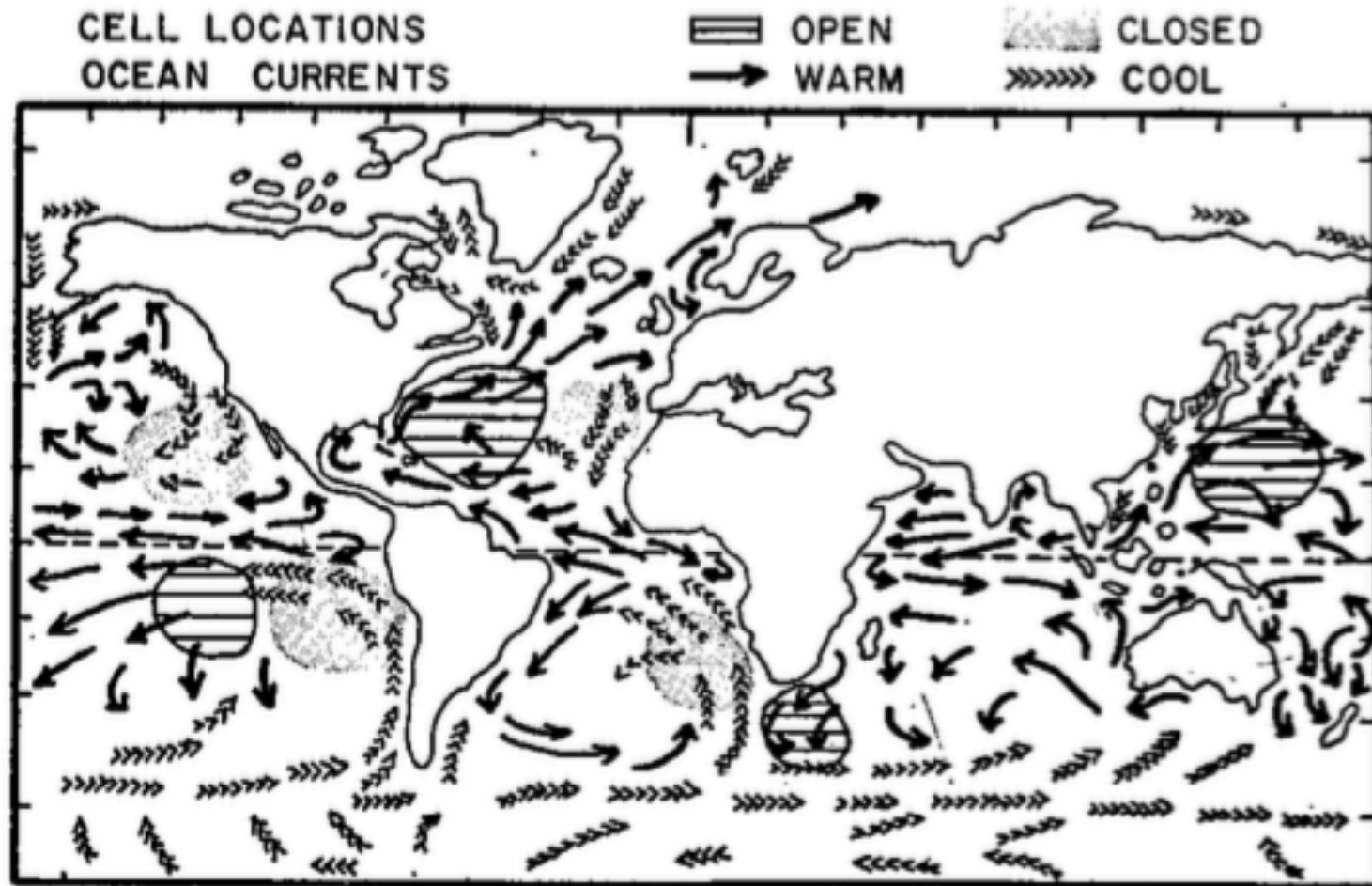
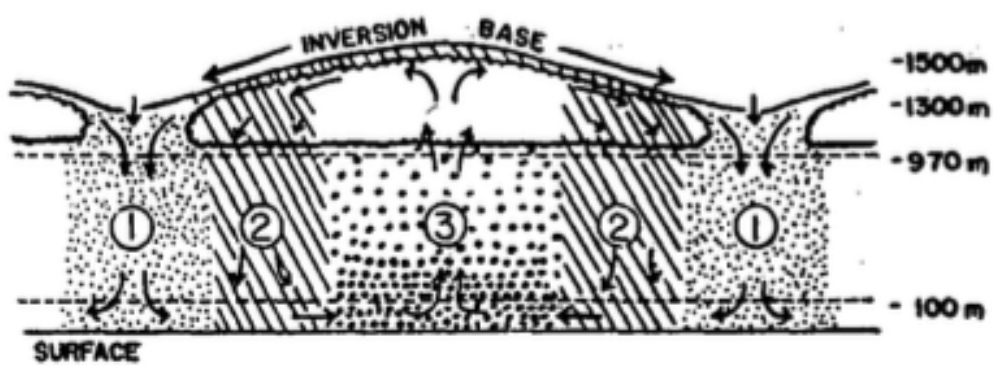
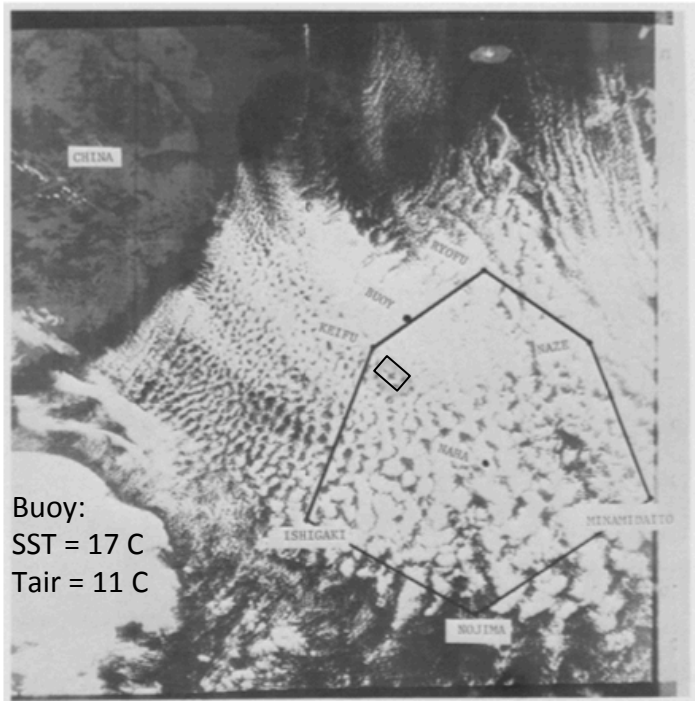


FIG. 3. A depiction of favored regions of open and closed cellular convection with respect to warm and cool ocean currents.

Agee et al. 1973 BAMS

AMTEX 1975



Rothermel and Agee 1980

Fig. 3a. DMSP satellite photograph of MCC patterns over the East China Sea and the AMTEX hexagonal network at 1155 JST 16 February 1975. The location of Buoy No. 10 is shown.

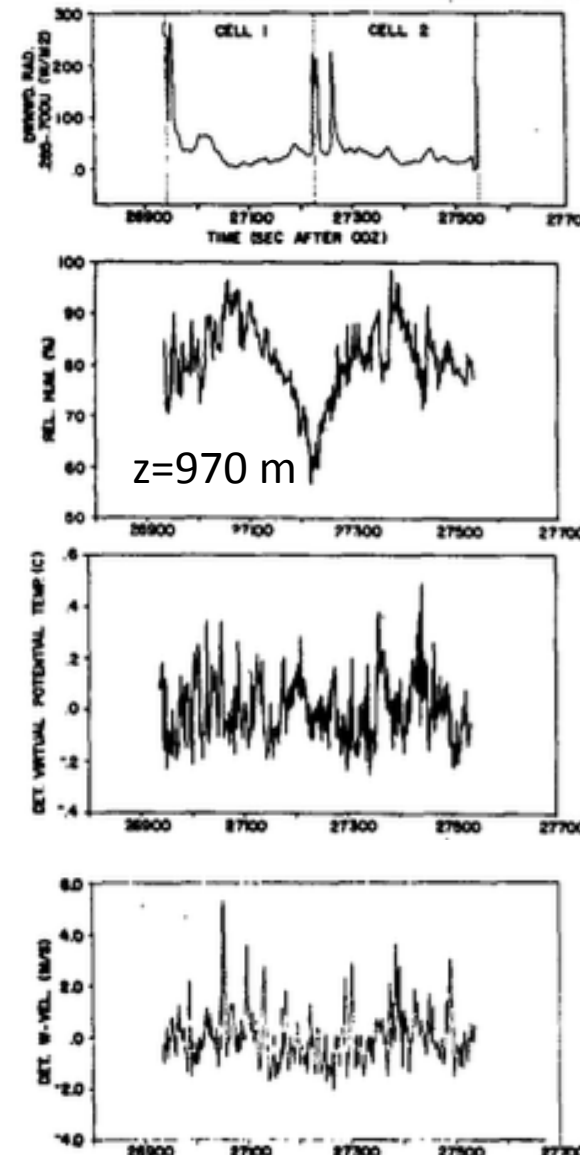
AMTEX Electra transects across closed cells just below cloud base

±10% mesoscale RH perturbations
~40 km wavelength (like clouds)

Weak buoyancy (θ_v) perturbations
below cloud base

Cumuliform-looking updrafts,
dominated by < 5 km scales

- Moisture and clouds have stronger mesoscale organization than do vertical velocity and buoyancy



Neural-net classification of MCC in MODIS imagery

(Wood and Hartmann 2006)

MCC type vs. inversion height

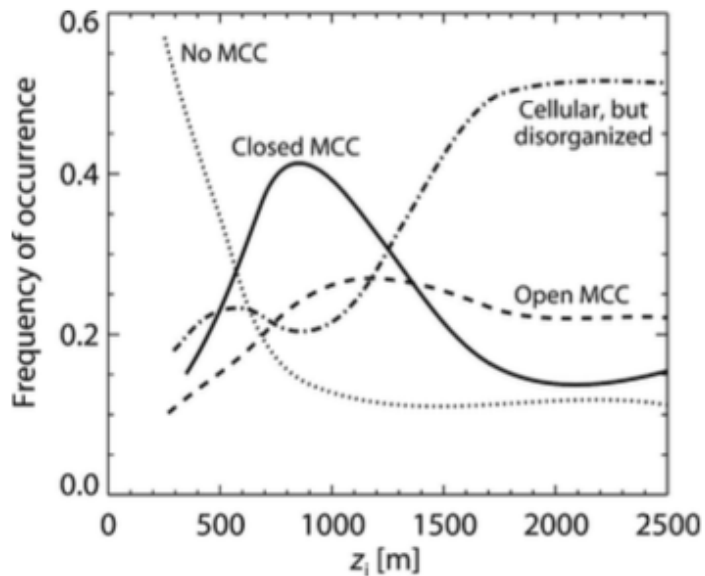


FIG. 16. Frequency of occurrence of the four scene type categories classified by z_p

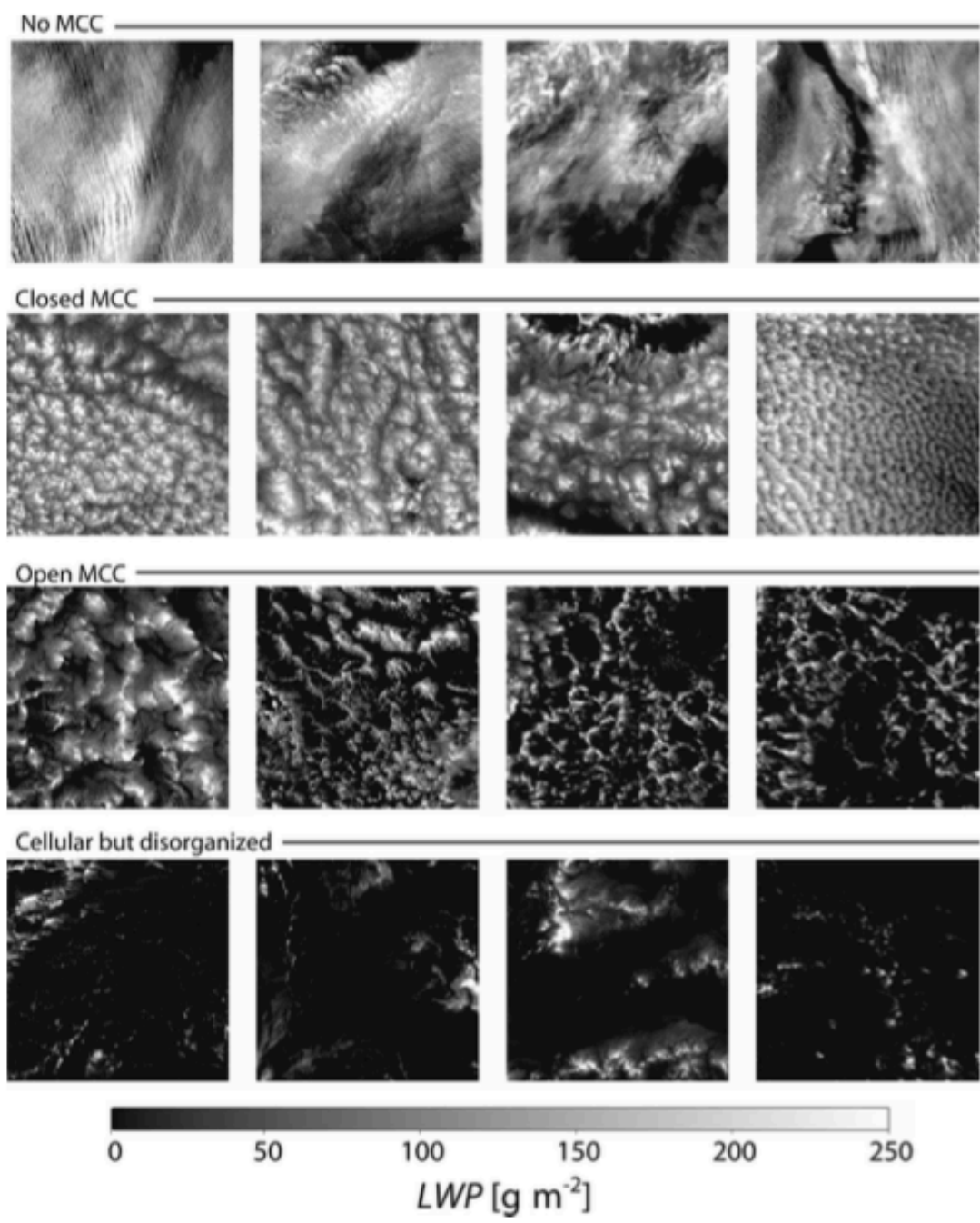


FIG. 5. Selection of MODIS scenes categorized by the neural network scene classification type.

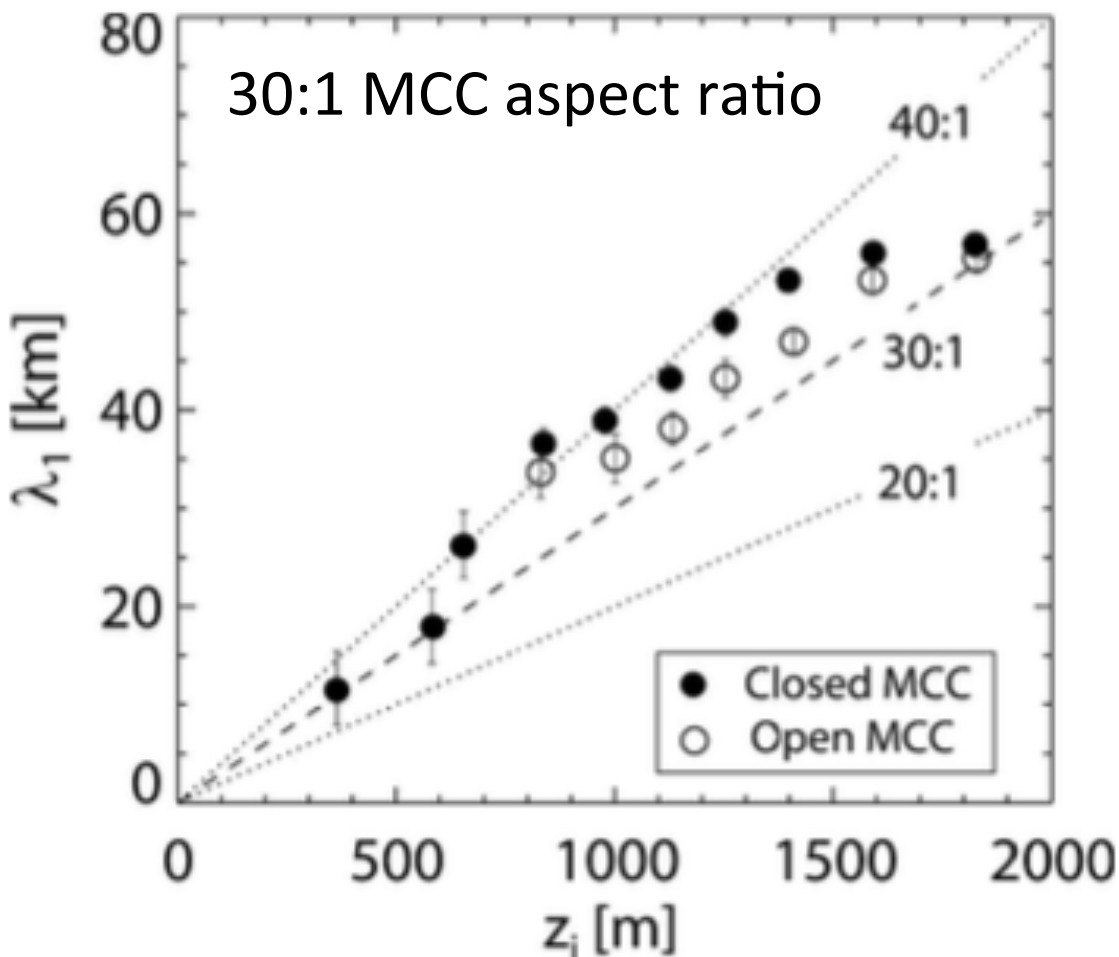
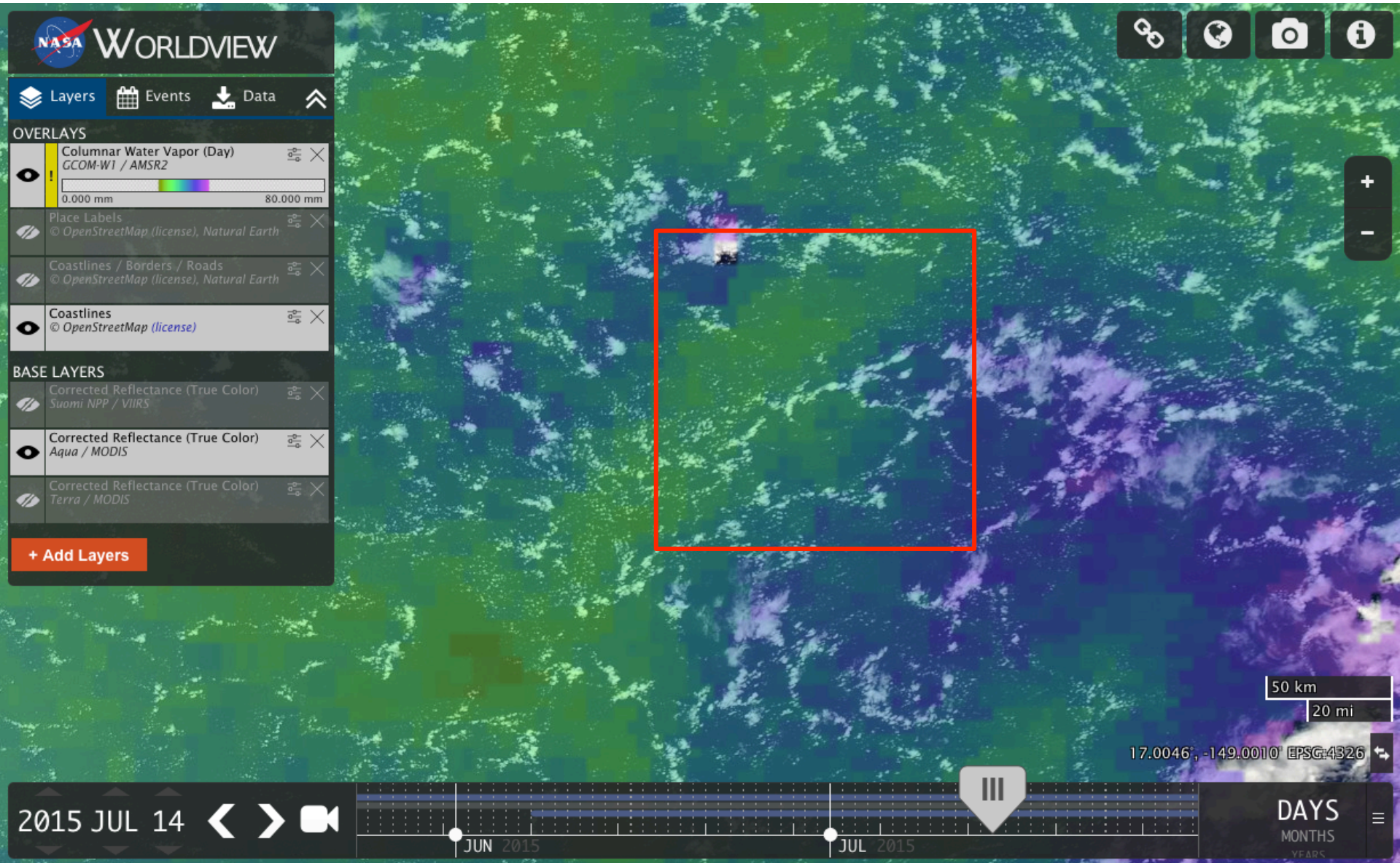


FIG. 17. Median characteristic cell length scale λ_1 binned by z_i for all MODIS scenes (solid circles) over the NE and SE Pacific. The dotted lines denote aspect ratios of 20:1, 30:1, and 40:1. Error bars indicate the approximate sampling error in the median. The solid line indicates the fit described in the text.

AMSR WVP and Aqua cloud imagery – clouds favor moist patches

Deepest cloud tops in image are at 3 km. WVP shading range = 30-45 mm



Large-eddy simulations and sensitivity studies

LES of MCC during ARKTIS

Mar 8 1991

Schroeter et al. 2005

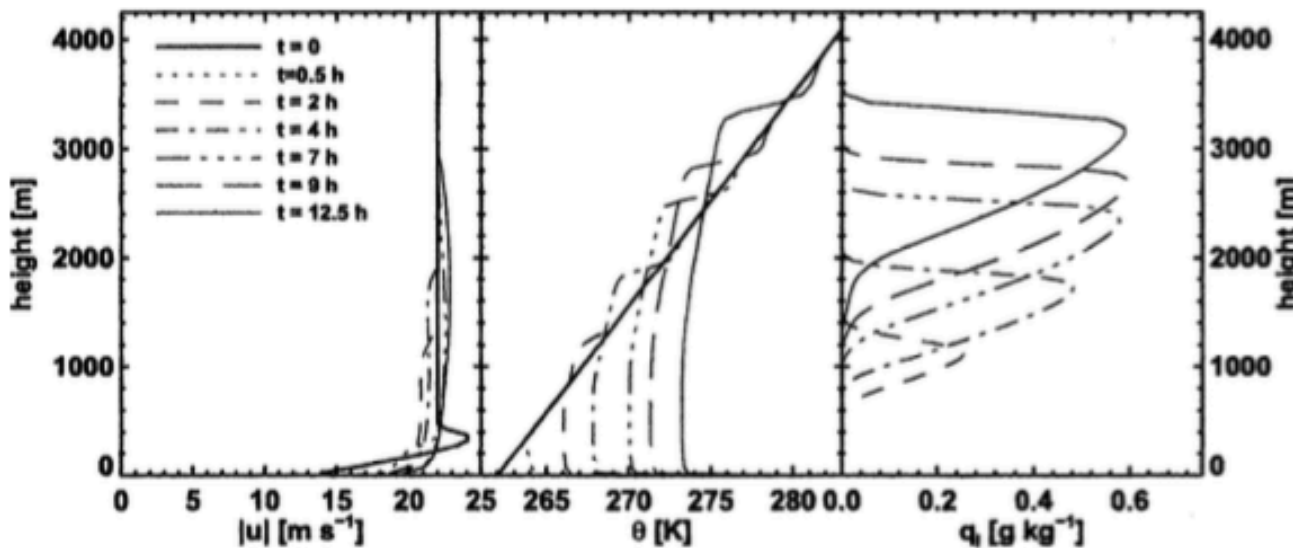
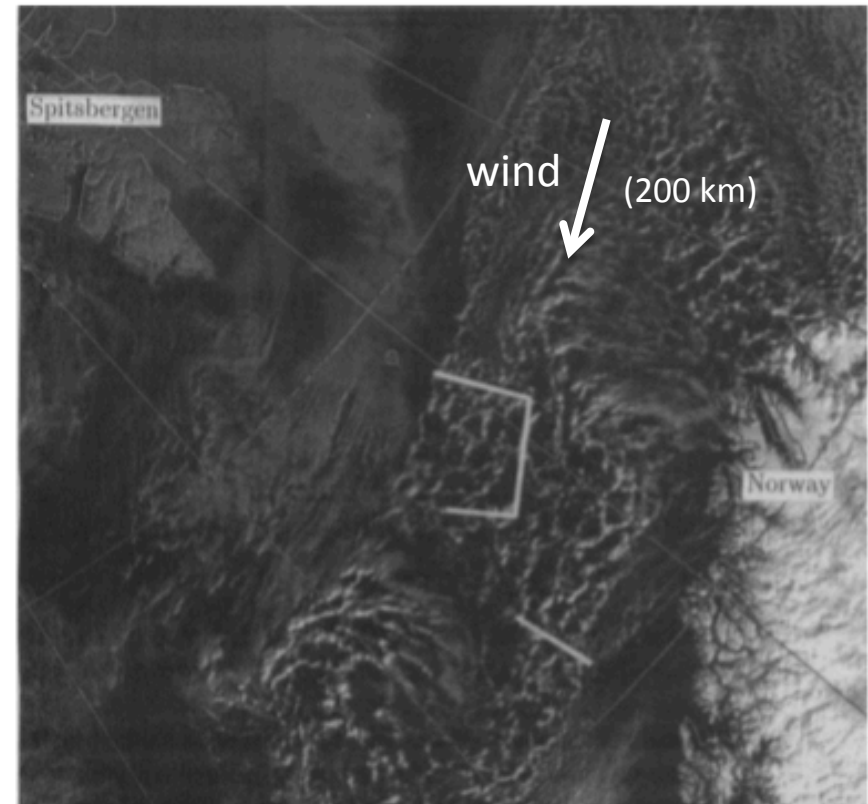
70.4 x 70.4 km domain

$\Delta x = 100 \text{ m}$, $\Delta z = 50 \text{ m}$

No ice

Specified rapidly-increasing SST

12.5 hrs = 900 km fetch



Cell aspect ratio goes from 5 to 11 over 12 hrs

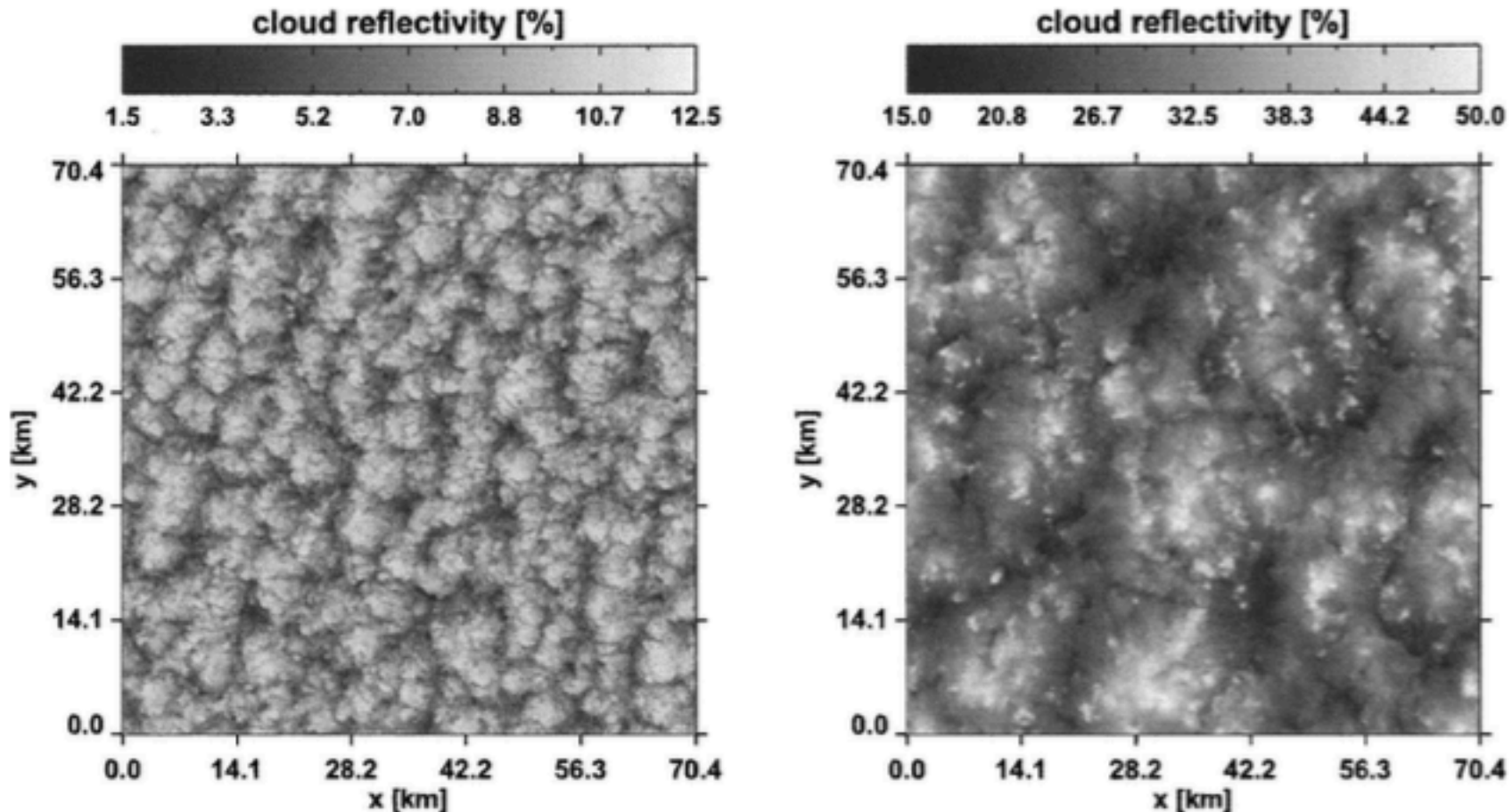
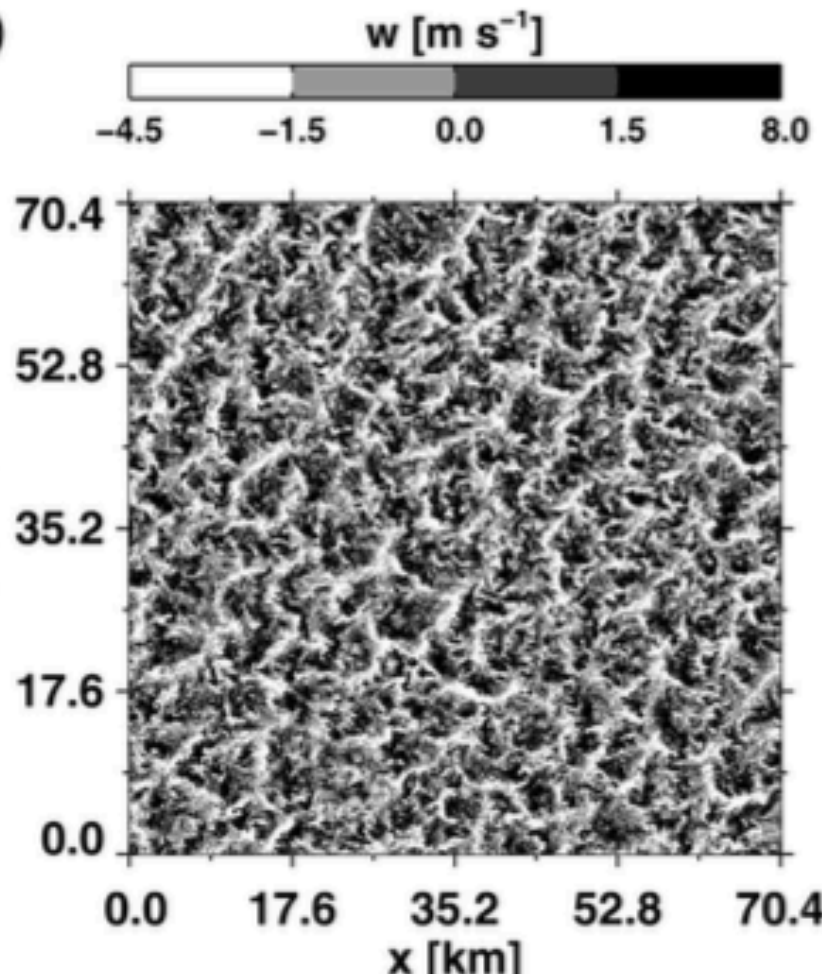


FIG. 2. Horizontal cross sections of cloud reflectivities calculated from the liquid water path (WET simulation): (left) $t = 4$ h, $z = 1600$ m; (right) $t = 12.5$ h, $z = 3100$ m. Cloud reflectivities have been estimated using the parameterization of Slingo (1989) assuming an equivalent radius of the drop size distribution of $6 \mu\text{m}$ and a solar zenith angle of 60° .

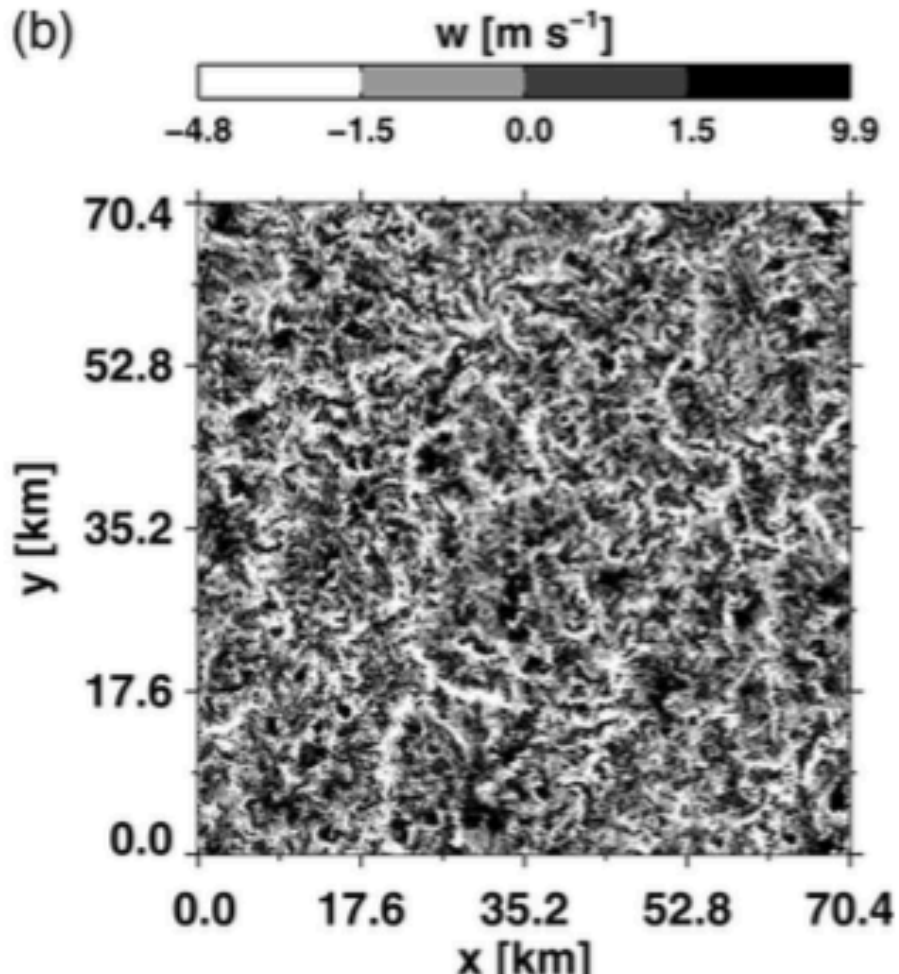
...but mid-PBL w is still dominated by small scales

(a)



4 hrs, $z=1300$ m

(b)



12.5 hrs, $z=2150$ m

Schroeter et al. 2005

Even with dry convection, passive scalars broaden somewhat

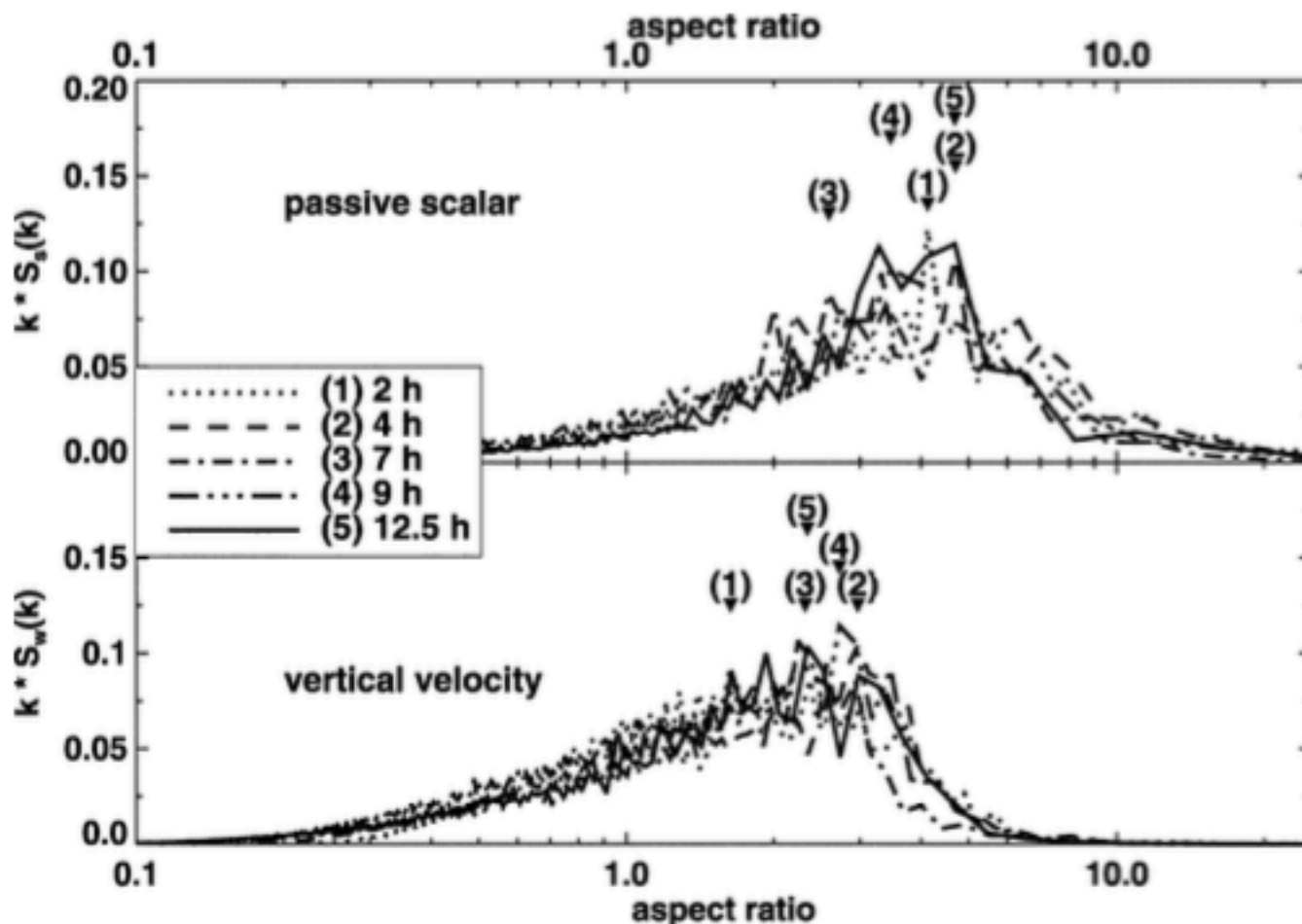


FIG. 6. (top) Power spectra of the passive scalar and (bottom) the vertical velocity, DRY simulation, resulting from two-dimensional Fourier analysis of horizontal cross sections located approximately in the middle of the developing cloud layer.

Schroeter et al. 2005, see also Jonker et al. 1999

But cell broadening stronger with radiation and latent heating

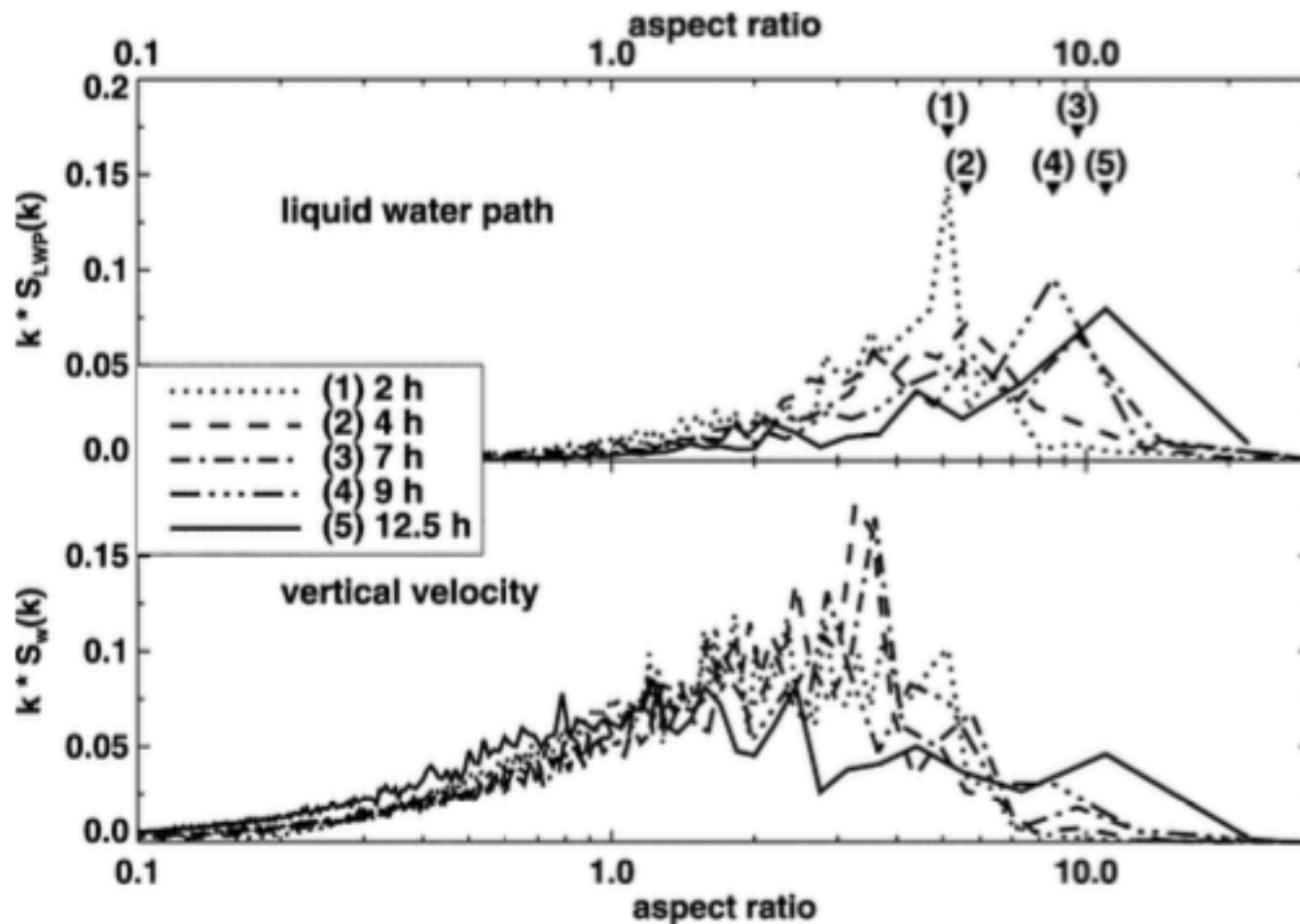


FIG. 4. (top) Power spectra of the liquid water content and (bottom) vertical velocity, WET simulation. Aspect ratios according to dominant scales at specific time levels are marked by triangles.

'Whereas on the scale of single coherent (e.g., up- and downdrafts) turbulent structures only the scalar variables show increasing aspect ratios, on the scale of MCC both dynamic and scalar field variables broaden because of a positive correlation between the thermodynamics and dynamics of the turbulent flow'

Schroeter et al. 2005

Closed cells broaden due to cloud-radiation interaction

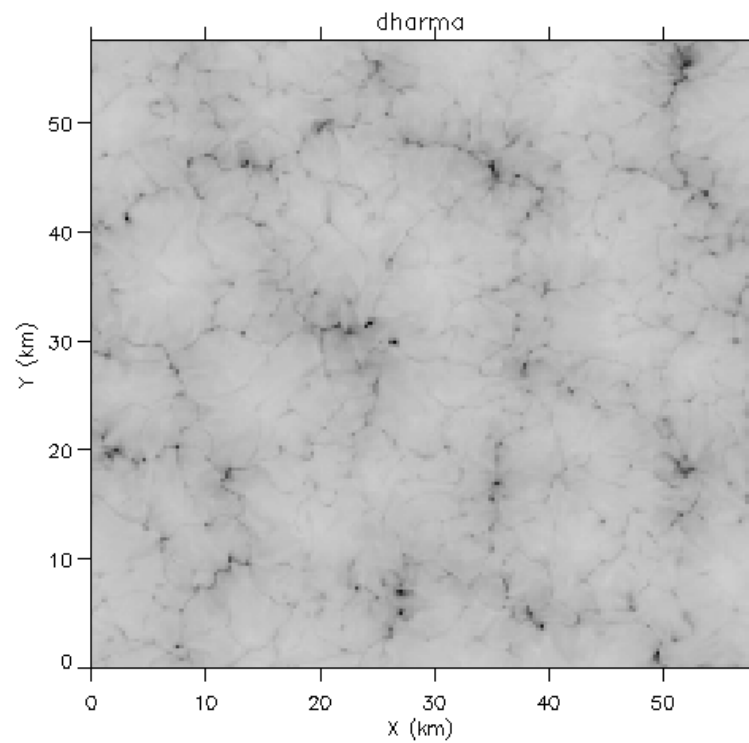
Zhou and Bretherton 2018

32 hrs, $z_i = 800$ m

Pseudo-albedo

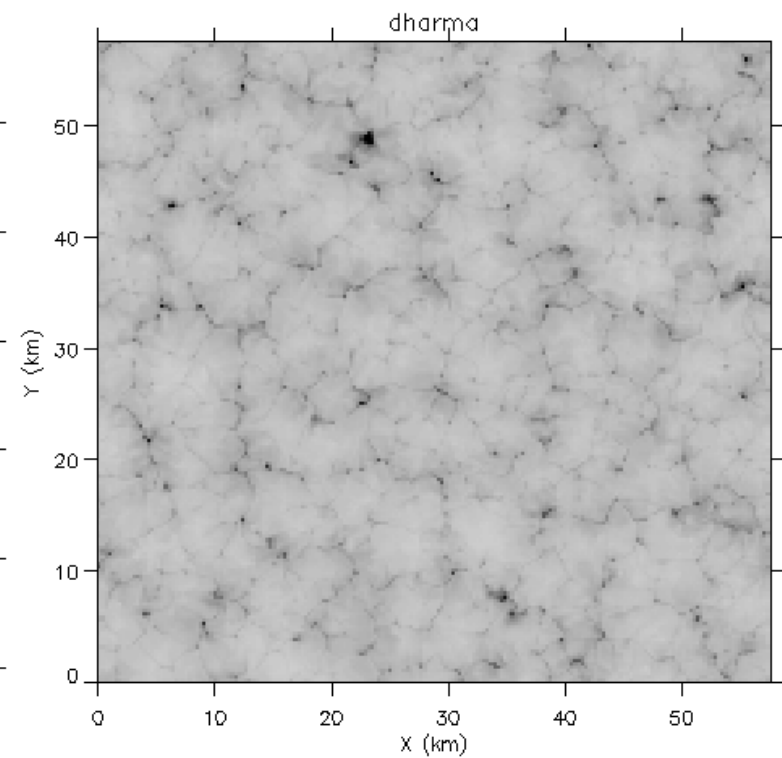
Interactive radiation

Cell broadening

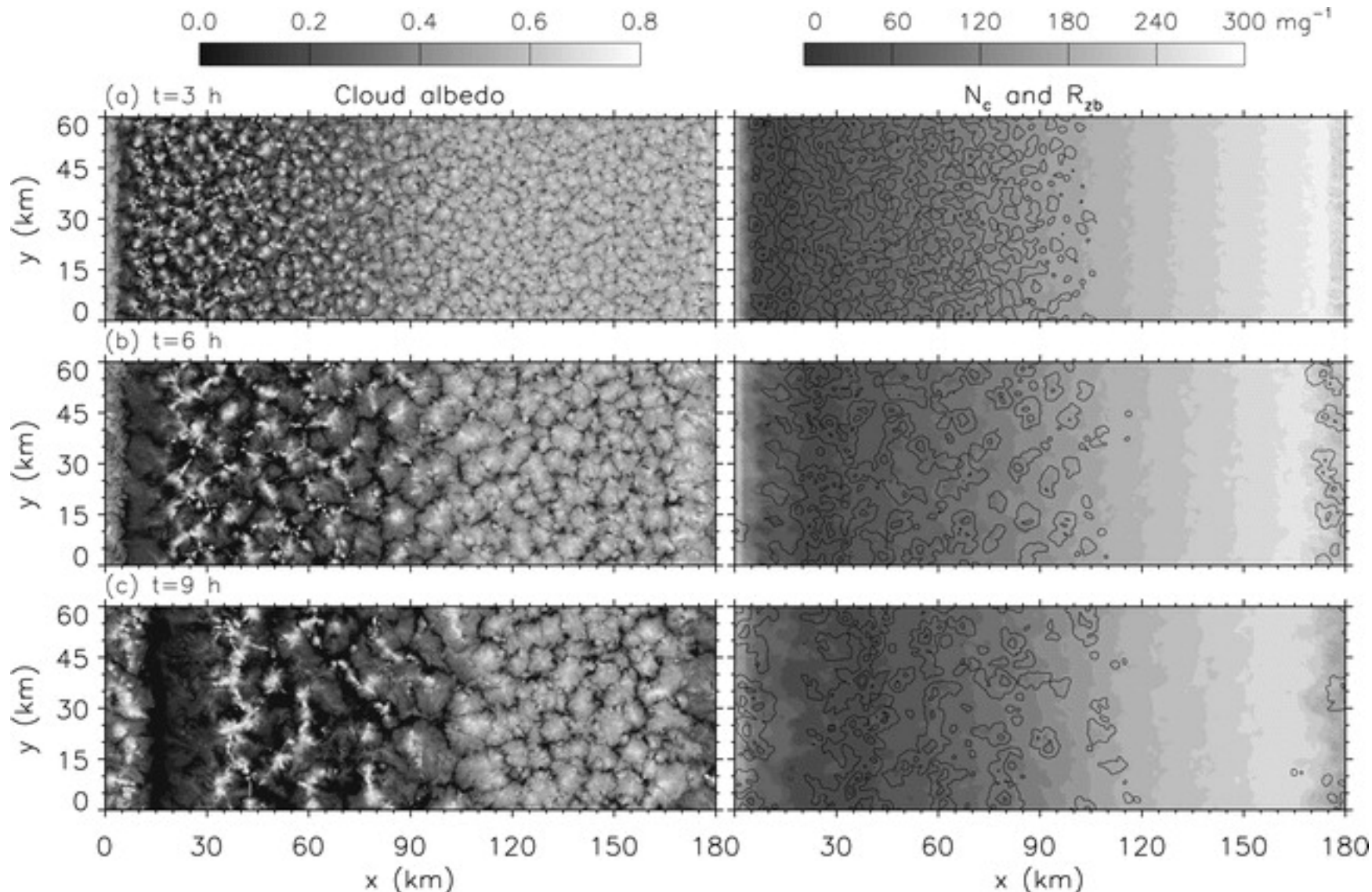


Homogenized radiation

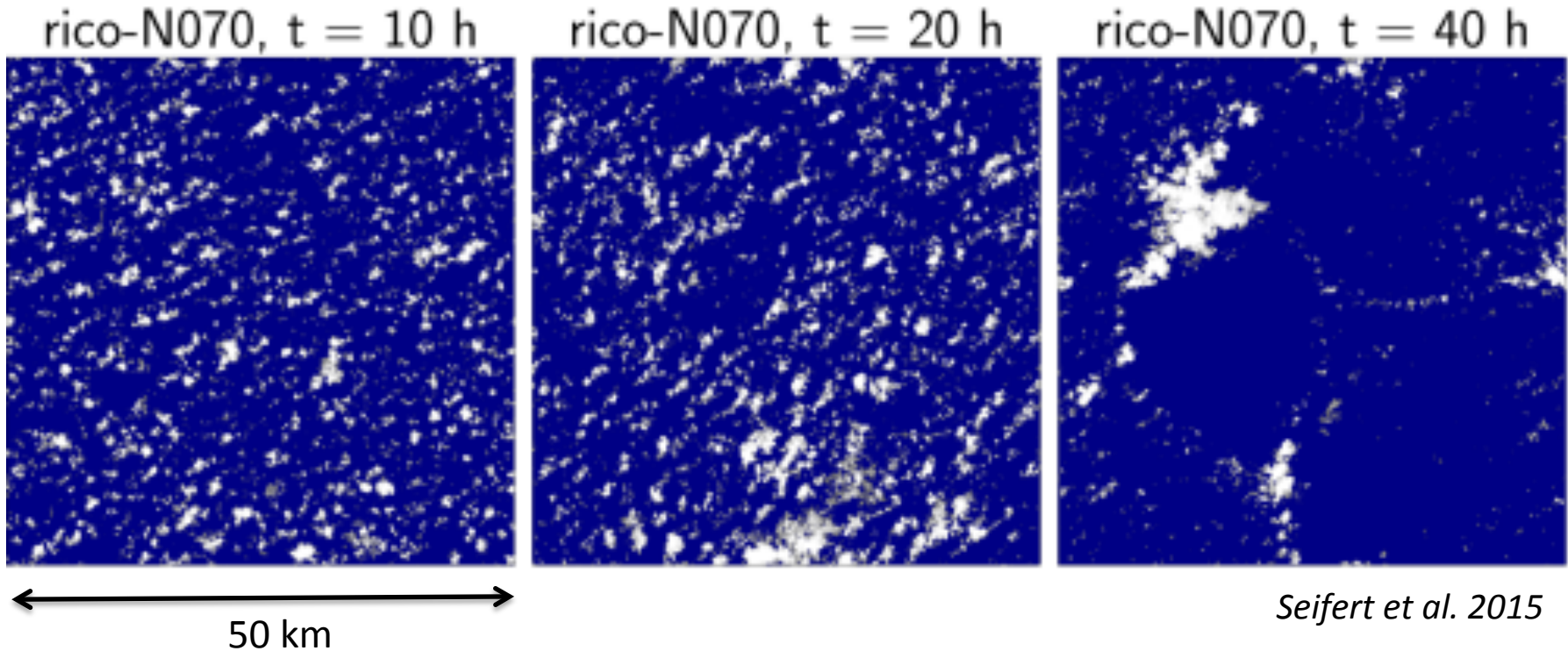
Much less cell broadening



Drizzle helps transition from closed to open cells



Aggregation of shallow cumulus

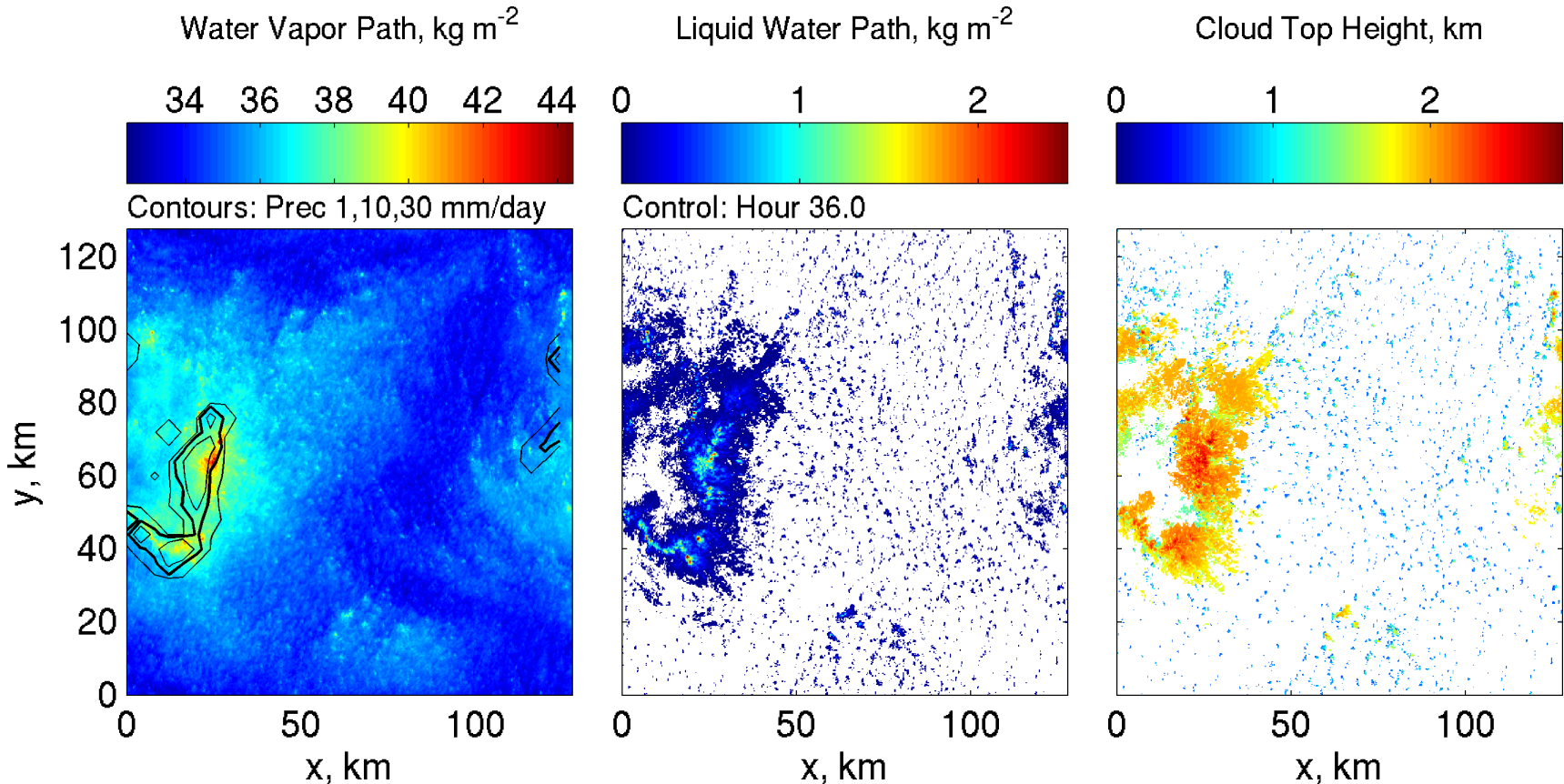


'It proves useful to distinguish among three stages in the temporal development of the simulations: (1) a non or very weakly-precipitating regime with no spatial organization of the cloud field; (2) a transition regime in which the rain rate increases and the cloud cover shows first an increase and then a rapid decrease; and (3) a quasi-stationary regime in which the cloud field is organized in mesoscale patterns.'

(isotropic 25 m grid spacing)

LES of shallow cumulus clustering

- SAM 6.10 LES, doubly-periodic $(128 \text{ km})^2$ domain, $\Delta x = 250 \text{ m}$, $\Delta z = 80 \text{ m}$
- Cloud droplet concentration $N_d = 100 \text{ cm}^{-3}$
- Initial profile: Homogeneous cumulus layer capped at 1.5 km by dry stable layer



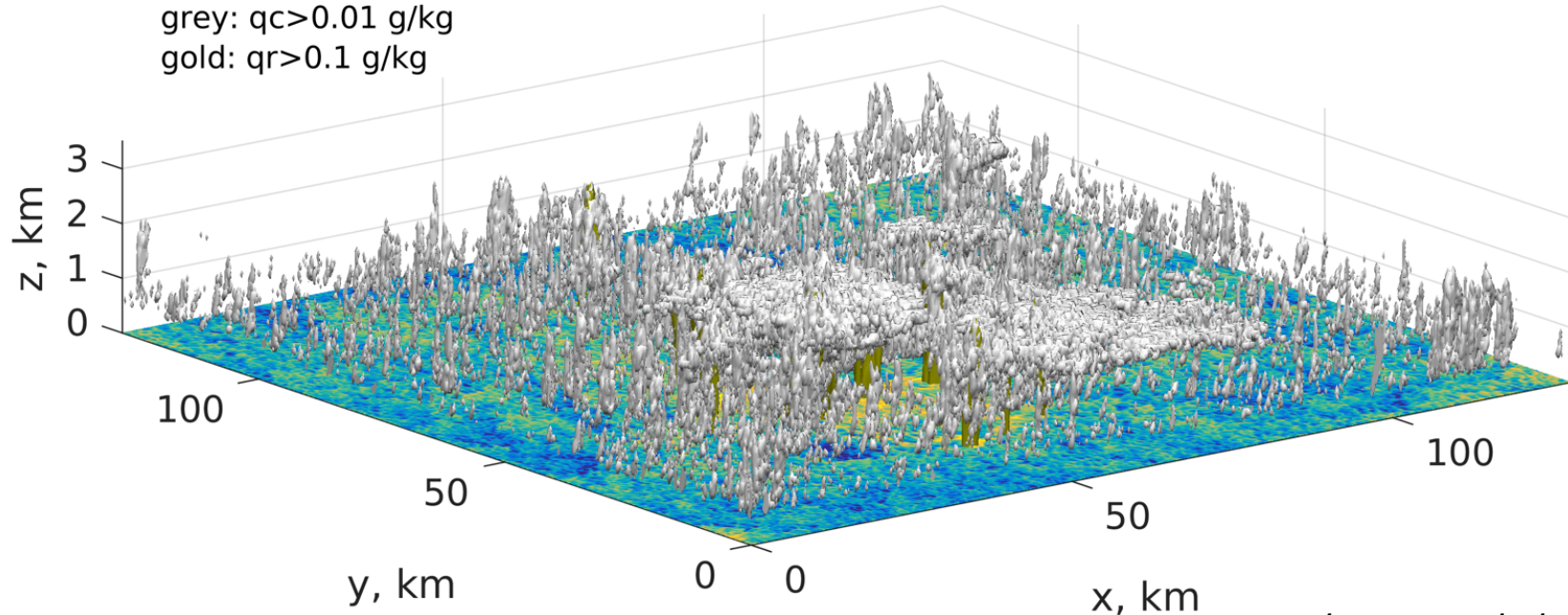
Bretherton and Blossey 2017

Cumulus clusters and veil clouds

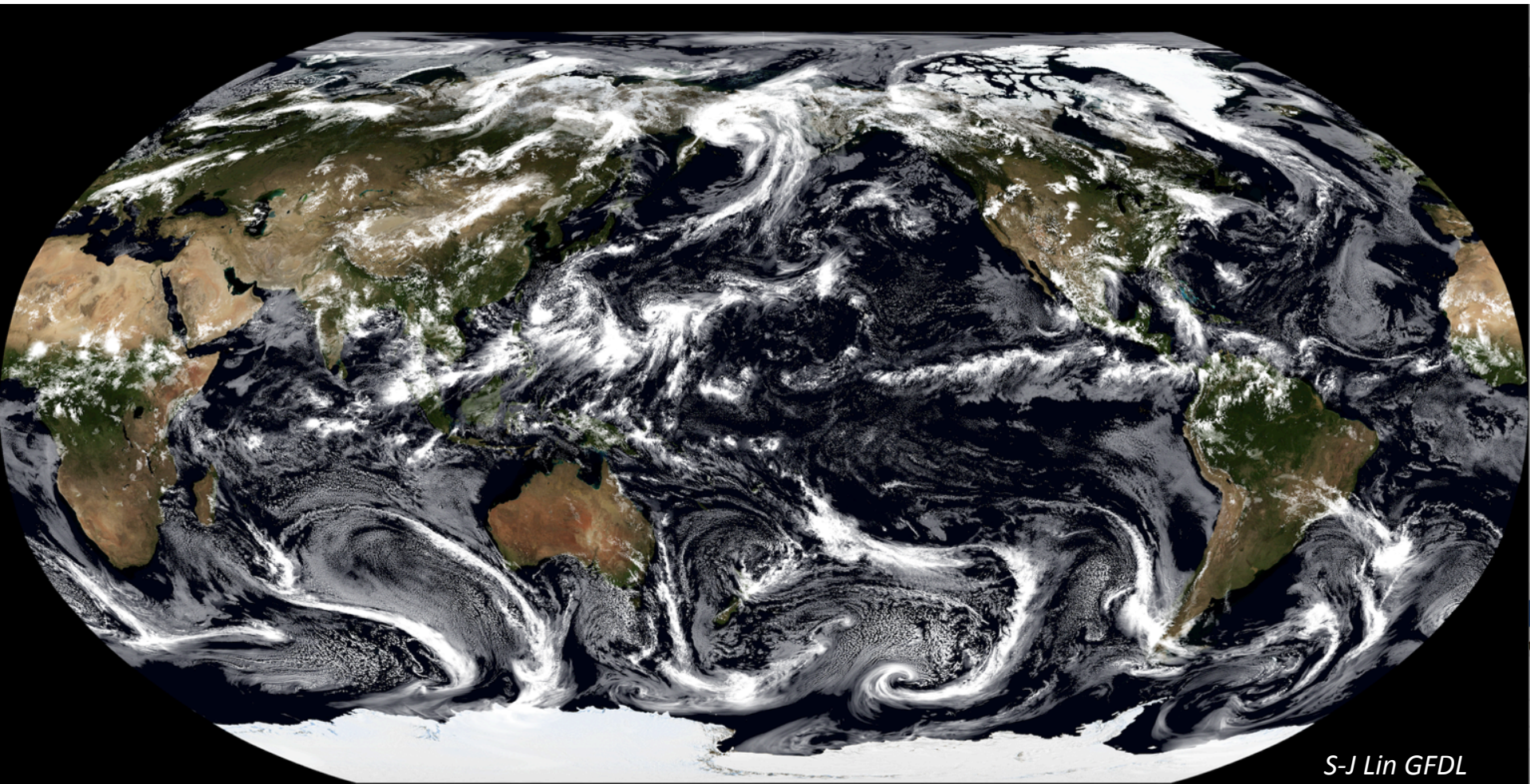


Large-domain LES → mesoscale Cu aggregation and veil clouds (even without precipitation)

Time = 32 hours
grey: $qc > 0.01 \text{ g/kg}$
gold: $qr > 0.1 \text{ g/kg}$



Mesoscale cellular cloud structure also apparent in global 3 km simulations

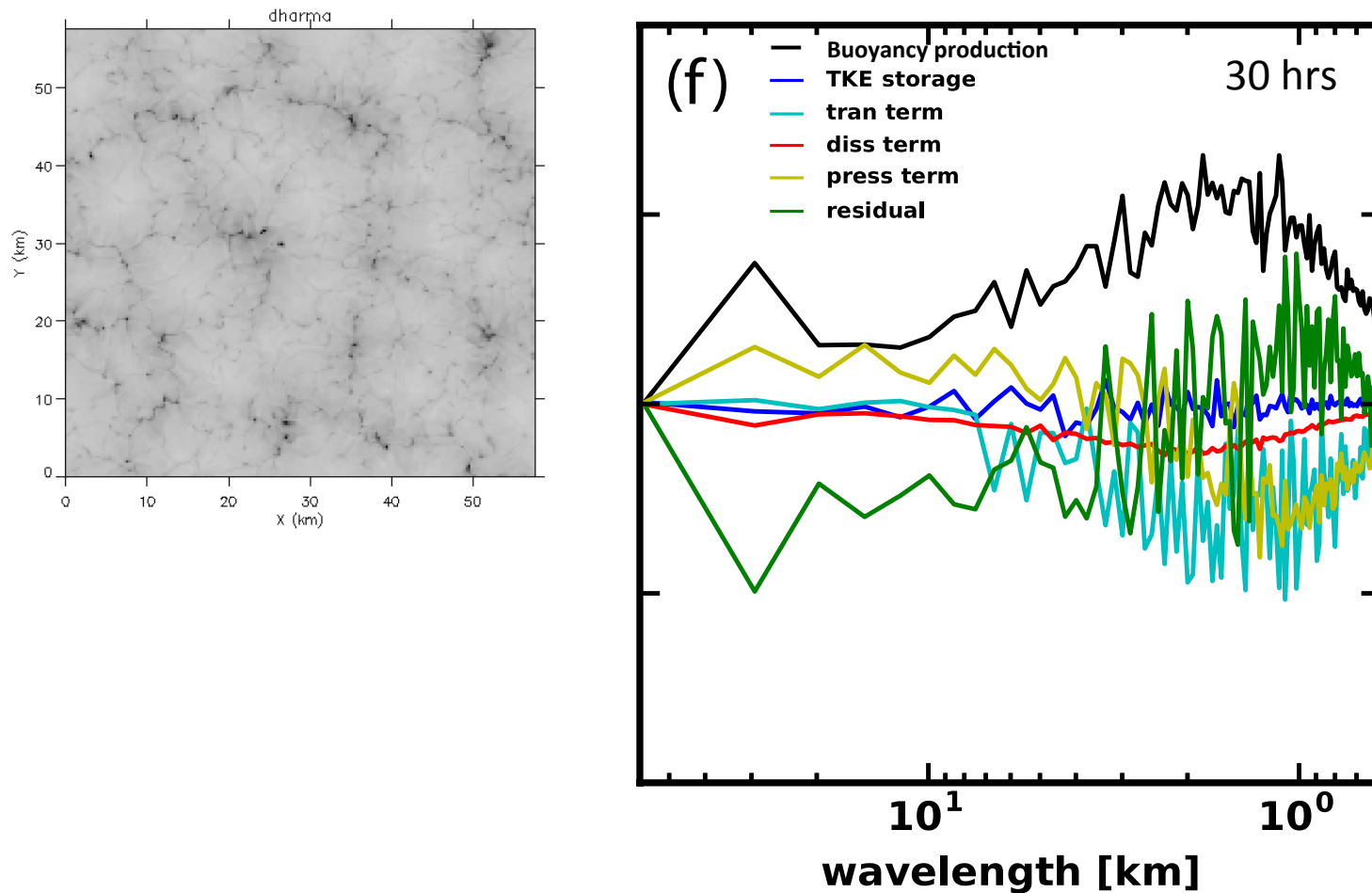


S-J Lin GFDL

Understanding

- Synthesis from LES
 - LES can simulate all types of mesoscale cellular convection
 - Mesoscale cellularity spontaneously develops in 12-24 hours and continues to broaden thereafter.
 - Vertical velocity variance remains concentrated on small scales
 - Mesoscale cloud patches collocated with high column-averaged humidity
 - Precipitation favors open-cell structure
 - Interaction of radiative cooling and cloud top needed for closed-cell structure
 - MCC is simulated even when boundary-layer turbulence is poorly resolved
- What generates broad cloud scales?
 - X Thermal convection with constant flux BCs or anisotropic eddy viscosity
 - Nonlinear variance/TKE transfer from smaller energy-generating scales?
 - Slow but persistent instability of longer-wavelength perturbations?

Direct buoyant TKE production at long wavelengths



...and TKE transfer seems to be downscale not upscale.

A long-wavelength humidity anomaly amplifies

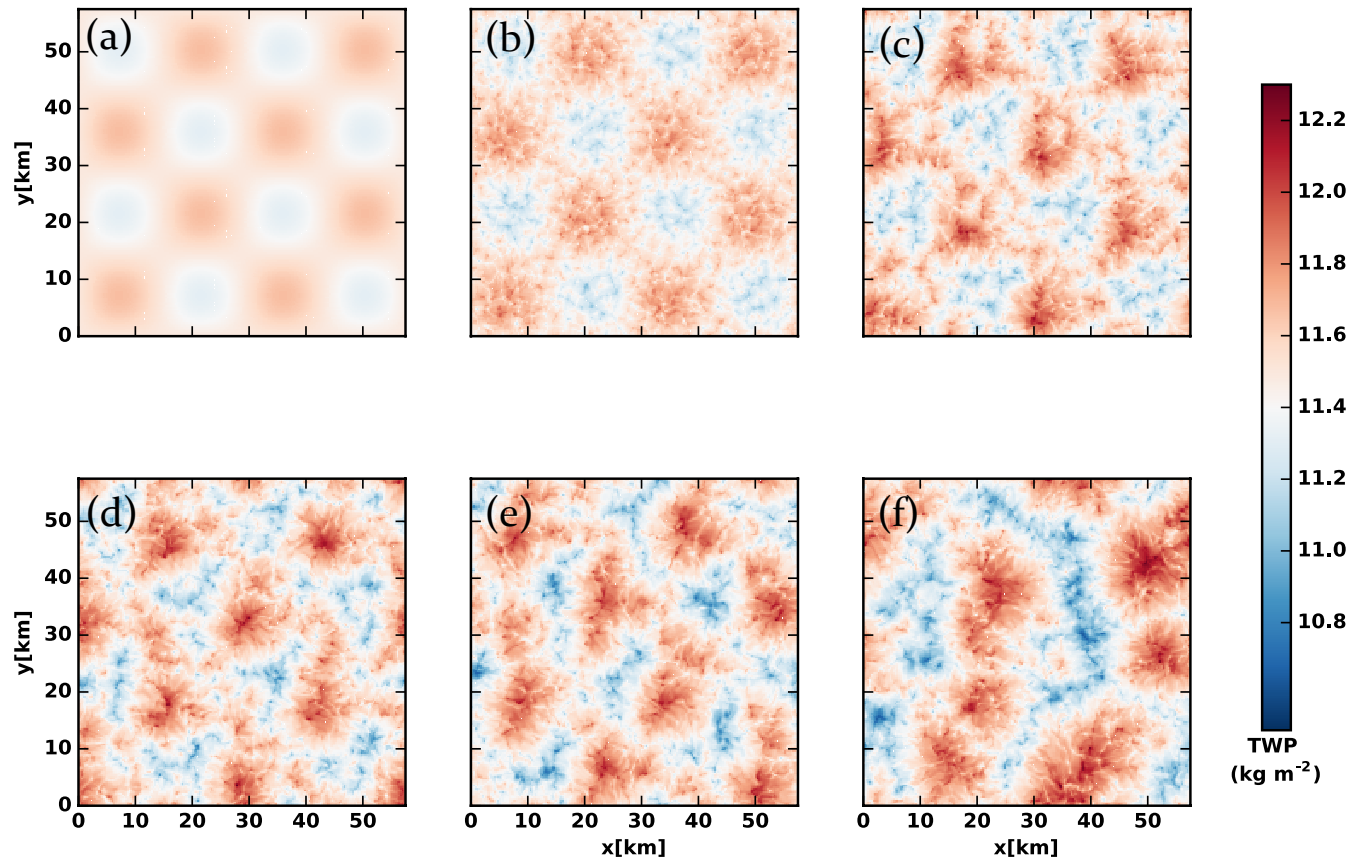
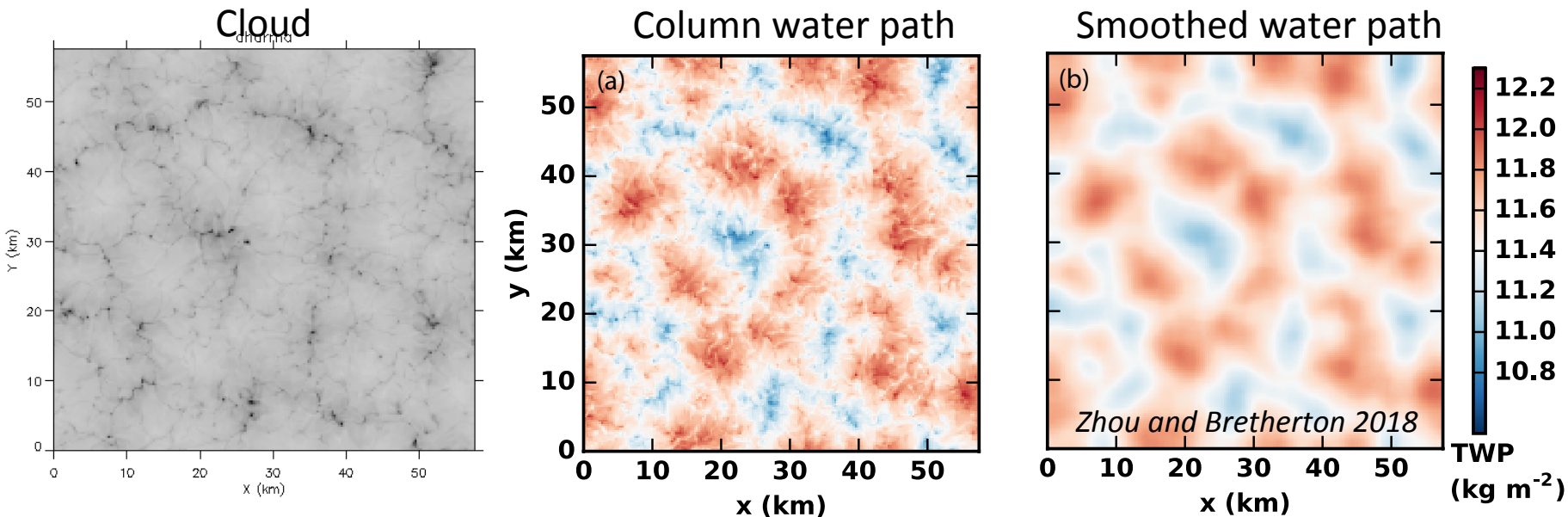


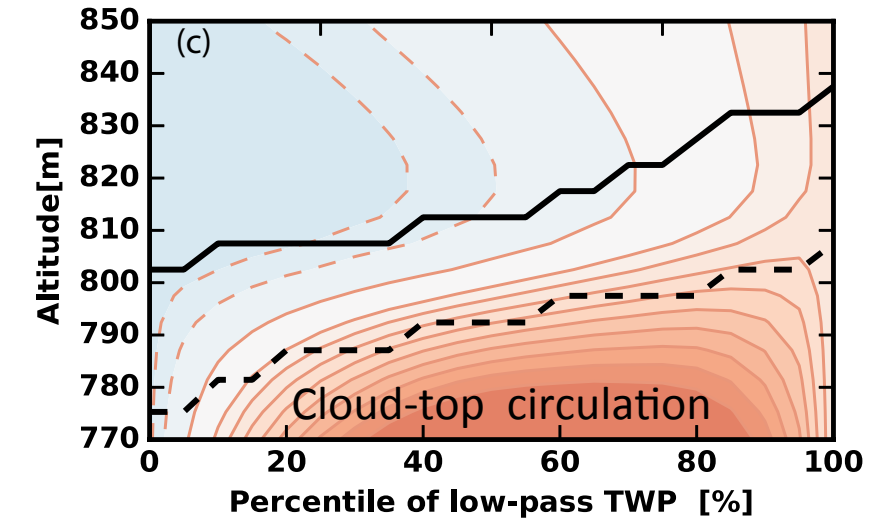
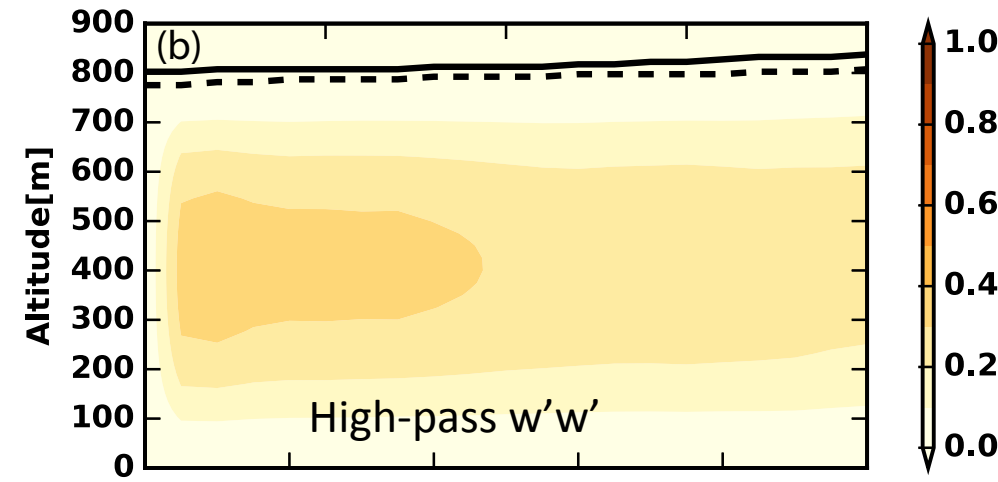
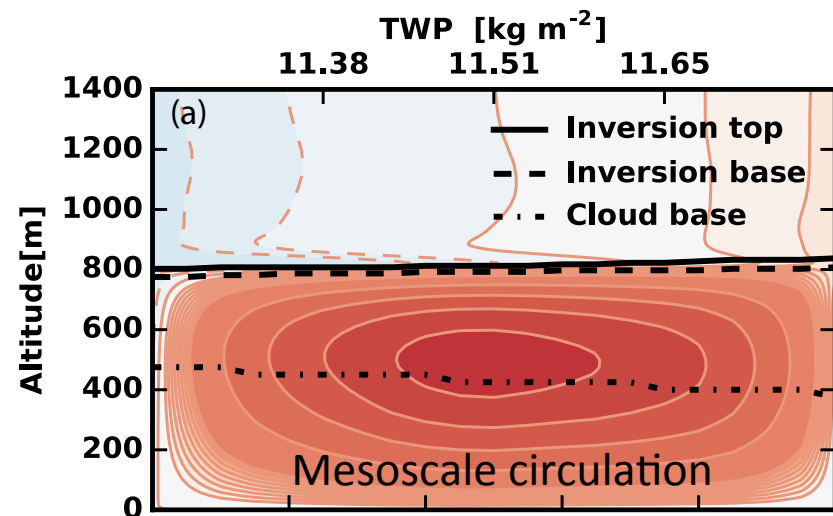
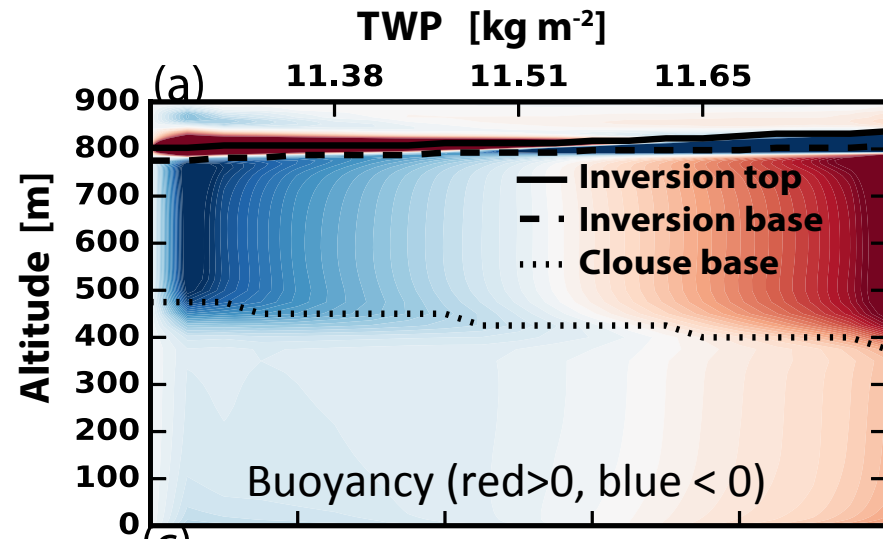
Fig. 4 Snapshots of total water path (TWP) for Nd500H initialized with a superposition of two-dimensional (horizontal) sinusoidal q_v perturbations at all levels in the STBL with spatial wavelengths of $\lambda m = 28.8$ km (half of the domain length L_x) and amplitudes of 0.2 g kg^{-1} . (a) 0 h, (b) 3 h, (c) 6 h, (d) 9 h, (e) 15 h, and (f) 30 h

Compositing based on column-integrated humidity

- LES suggest that mesoscale cloud organization is strongly correlated with mesoscale-smoothed (*) column water path
$$W = \int_0^H \rho q dt dz$$
- We order W^* of grid columns from driest to moistest and composite by binning into quartiles or percentiles, following Bretherton et al. (2005).



A composite closed cell

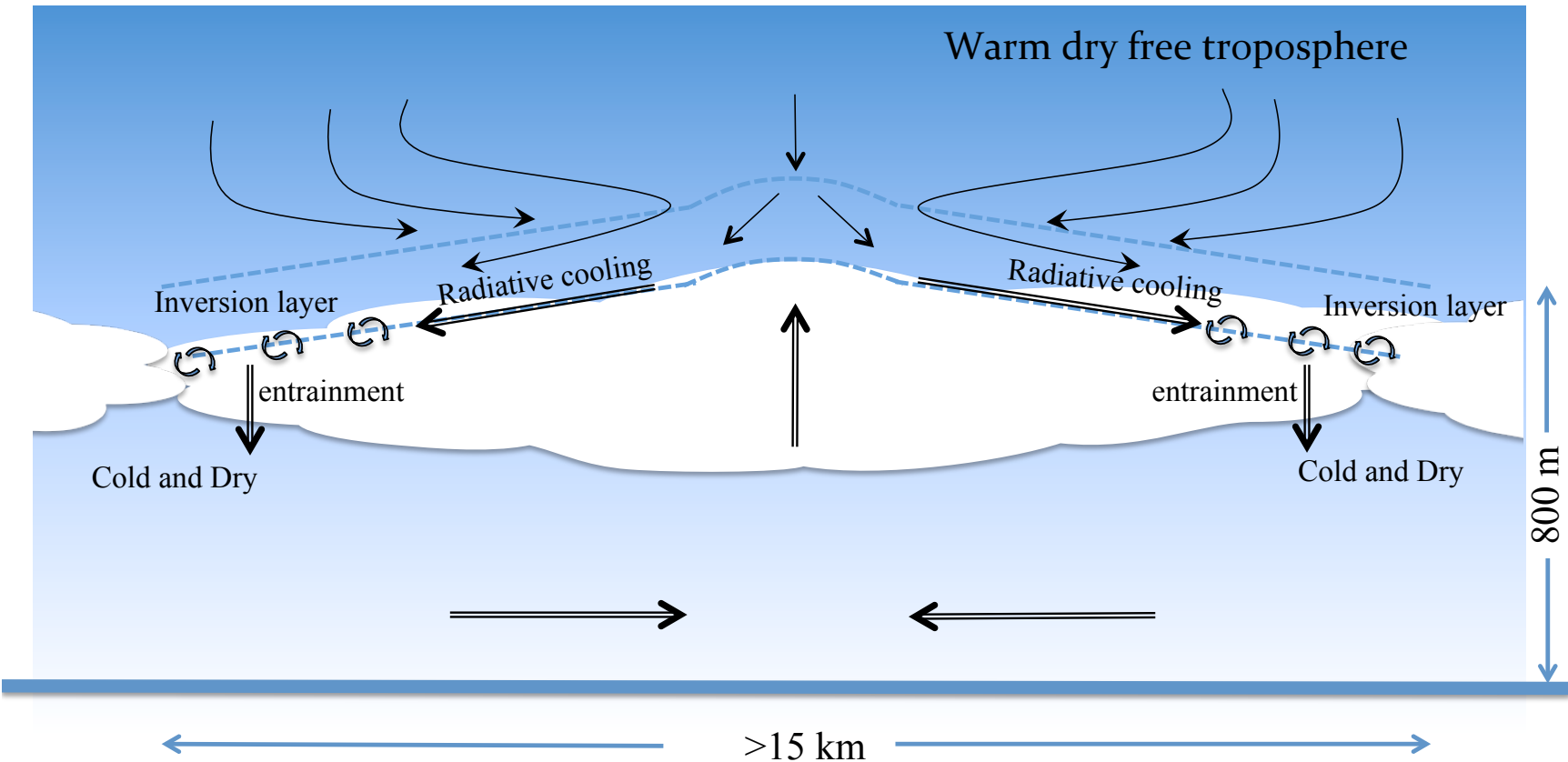


Thermally direct, vertically well mixed in PBL

More entrainment in dry regions

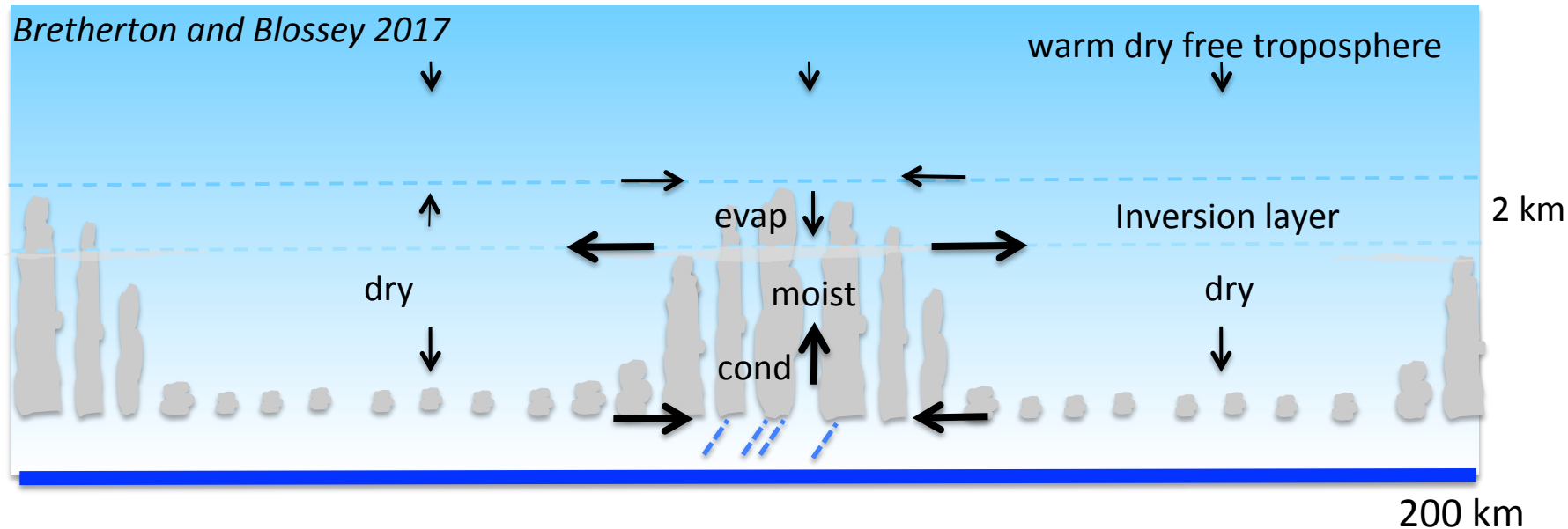
Longwave cooling helps air slide down sloped inversion

Composite-based schematic of closed-cell convection



- Buoyant updrafts in moist, cloudy regions
- Entrainment driven by stronger turbulence preferentially dries the dry regions
- Cloud-top radiative cooling of air sliding down inversion from moist to dry region
- Net result: Moist regions moisten and warm relative to dry regions, amplifying the humidity anomalies

Shallow cumulus: circulations and moisture aggregation



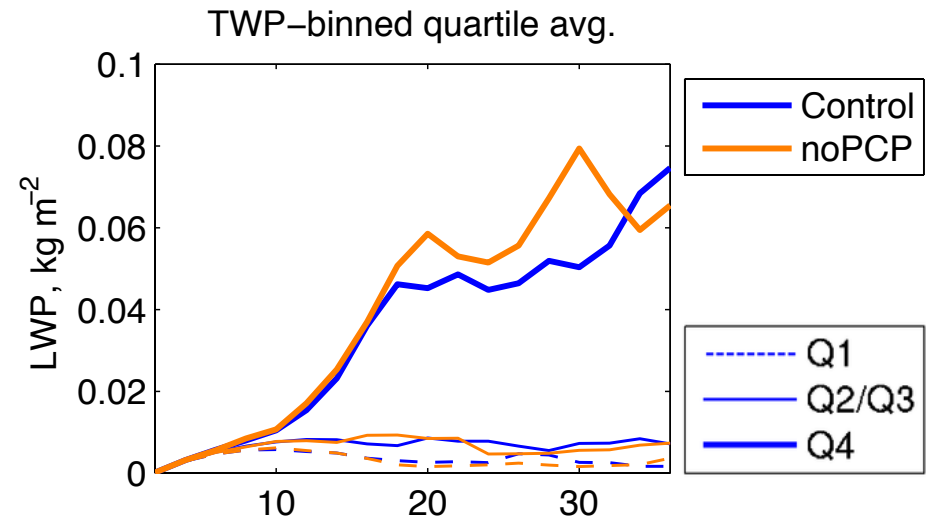
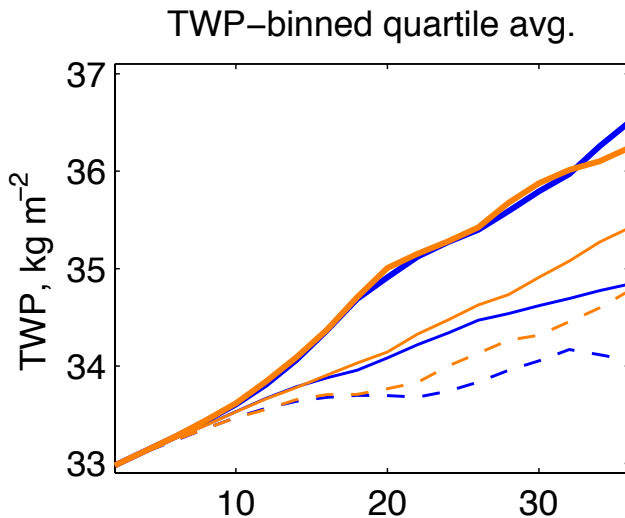
- Negligible horizontal temperature gradients (stratified adjustment)
- Moister columns convect more and deeper
- This produces apparent heat and moisture sources on mesoscale
- The Cu heat source induces mesoscale upward motion
- Low level moisture convergence further moistens column, despite more Cu entraining more dry warm air from free troposphere

Synthesis

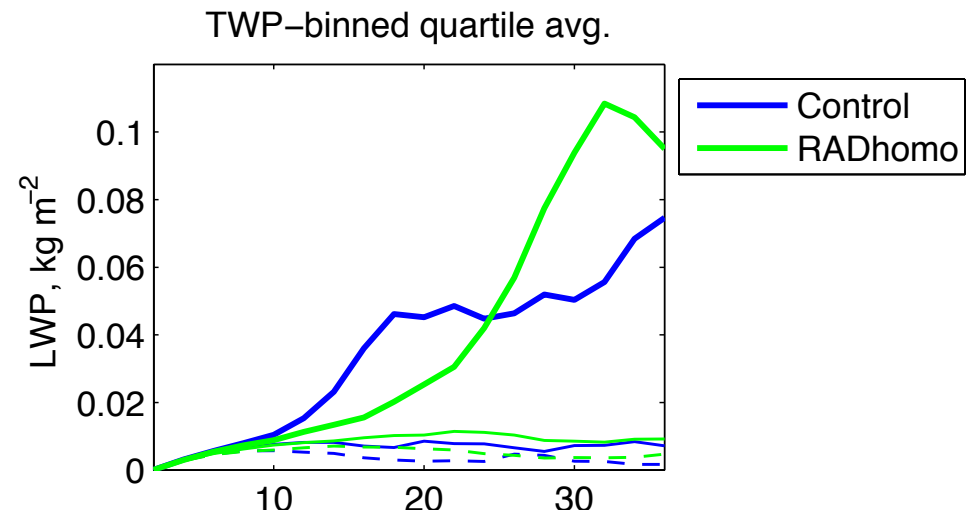
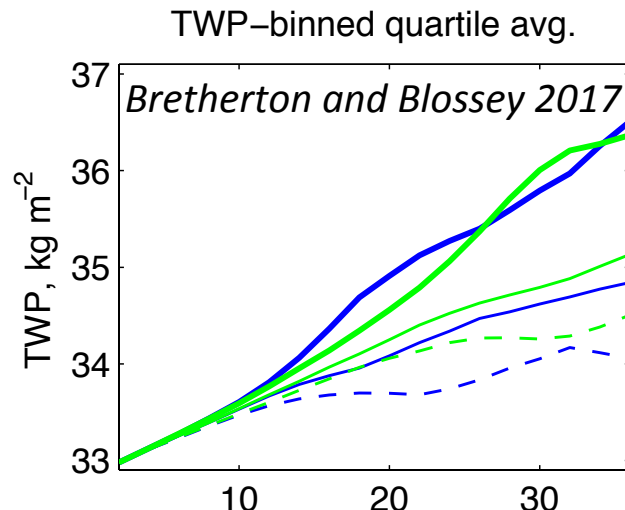
- Mesoscale boundary layer cloud organization is ubiquitous
- Even a passive tracer in a convective boundary layer will tend to develop variance at broader scales, but cloud-radiation interaction and latent heating/precipitation feed back positively
- Can be regarded as a long-wavelength instability in which moist and dry anomalies amplified by their induced circulations.
- Column humidity compositing helps visualize this process.

Sensitivity studies

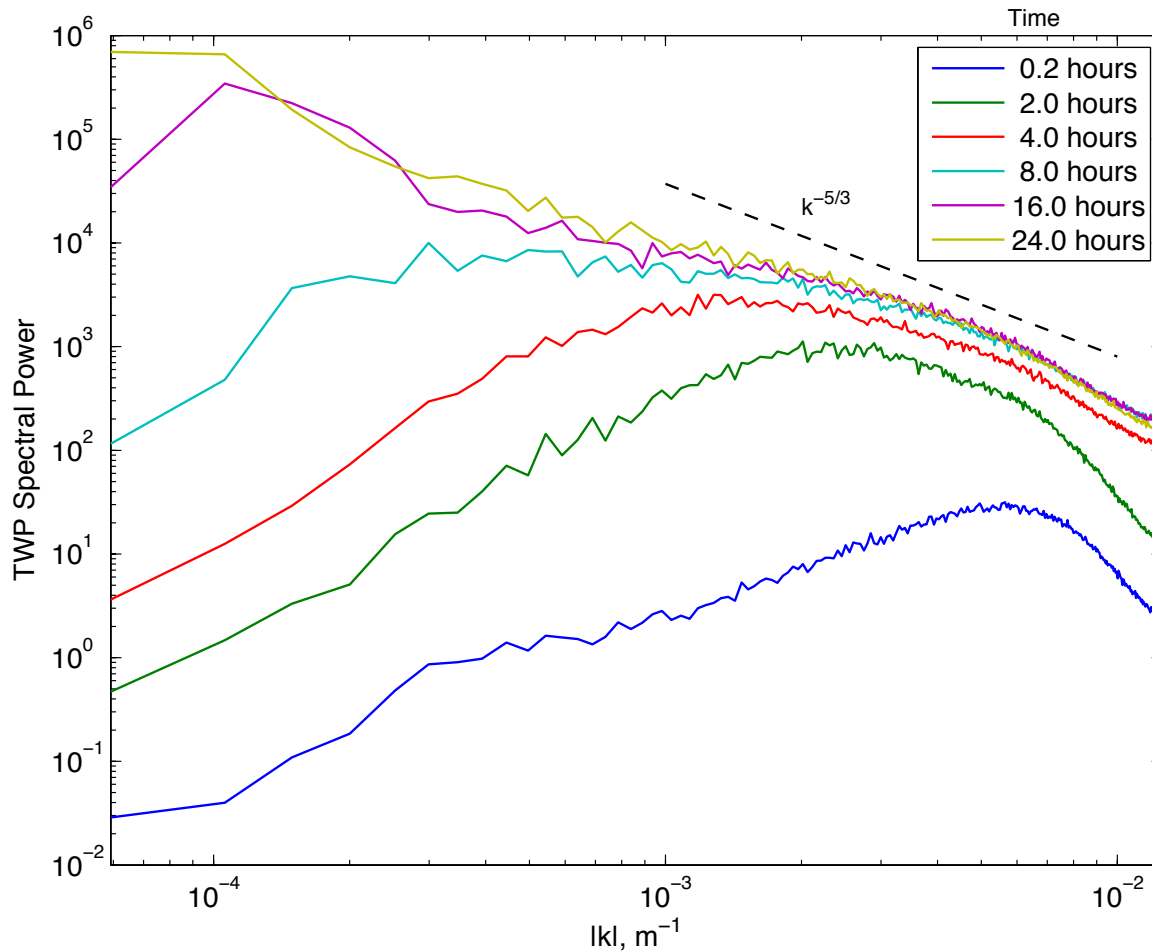
No precipitation → similar aggregation



Horizontally homogenized radiation → slower aggregation



Control run TWP spectral evolution



Short wavelengths quickly nonlinearly saturate, longer wavelengths keep growing